The Thesis Committee for Eugen Petrut Tudor
Certifies that this is the approved version of the following thesis:

FACIES VARIABILITY IN DEEP WATER CHANNEL-TO-LOBE TRANSITION ZONE:

JURASSIC LOS MOLLES FORMATION, NEUQUEN BASIN ARGENTINA

APPROVED BY

SUPERVISING COMMITTEE:

Supervisor:

Ron Steel

Co-Supervisor:

Cornel Olariu

David Mohrig

FACIES VARIABILITY IN DEEP WATER CHANNEL-TO-LOBE TRANSITION ZONE: JURASSIC LOS MOLLES FORMATION, NEUQUEN BASIN ARGENTINA

by

Eugen Petrut Tudor, B.S.c

Thesis

Presented to the Faculty of the Graduate School of

The University of Texas at Austin

in Partial Fulfillment

of the Requirements

for the Degree of

Master of Science in Geological Sciences

The University of Texas at Austin

May 2014

Dedication

To my loving family and friends who offered me unconditional support throughout my stay in the United States.

Acknowledgements

Thank you to my supervisors, Ron Steel and Cornel Olariu for finding me in Romania and setting a path for me to follow in the world of geosciences. I will always be grateful for helping me to pursue and receive a degree from UT Austin. Thank you for the fruitful discussion and encouragement, for helping me in the field, for teaching me to be skeptical of everything.

I recognize and appreciate the financial support offered by Statoil SA through their financial support (Channel to Lobe Research Grant UT Austin) and important feedback, especially Mason Dykstra. I appreciate the technical advice and guidance from experienced professionals and colleagues, David Mohrig and Mauricio Perillo.

Thank you, Nateleigh Vann, Rene Winter and Moonsoo "Brian" Shin for your help and company during field seasons in Alumine, Argentina.

Thank you, Rattanaporn Fongngern for always arguing with me for the right reasons and accepting me to be your field assistant for two seasons.

Finally, I am grateful for the great debates within the Dynamic Stratigraphy Research Group (Josh Dixon, Michael Cloos, Valentina Rossi, Julio Leva, Yu Ye and everyone else) from The University of Texas at Austin.

Abstract

FACIES VARIABILITY IN DEEP WATER CHANNEL-TO-LOBE TRANSITION ZONE: JURASSIC LOS MOLLES FORMATION, NEUQUEN BASIN ARGENTINA

Eugen Petrut Tudor, MS Geo Sci

The University of Texas at Austin, 2014

Supervisors: Ron Steel and Cornel Olariu

This study focuses on the facies changes from the lower slope to toe-of-slope to basin floor over a 10 km outcrop belt, in down-dip and oblique-strike directions to the basin margin. The Jurassic Los Molles Formation in Neuquen Basin, Argentina represents the slope and basin floor of basin margin clinoforms, coeval with the shallow water and fluvial deposits named Las Lajas and Challaco formations respectively. The shallow and deep water deposits are diachronously linked in an Early-Mid Jurassic source-to-sink system developed in a back-arc basin during the incipient development of the Andes Mountains. Satellite images, high resolution panorama pictures and measured sections were used to correlate and interpret the spatial variability and overall geometry

of the base of slope to basin floor units. The observations of this study refine the model for the channel-to-lobe transition zone with increase recognition and quantification of facies and architecture variability. The Los Molles basin margin was coarse grained and was ideal to observe changes in the geometry and depositional facies of channel-to-lobe deposits from updip to downdip continuous over an 8 km outcrop belt. The described channel-to-lobe transition zone clearly shows a downdip change in bed boundaries from dominantly erosive to non-erosional (bypass) to depositional and with a range of distinct facies changes. In the transition zone the sand to shale ratio is high (N:G: 65-70 %), with gutter casts and deep scours, with a high degree of amalgamation, gravel lags, mud rip-up clasts and laterally migrating beds. Within the same depositional unit (deep water lobe), at the base of the slope, the dominant sandstone beds change from amalgamated structureless and normal graded sandstone beds in the channelized lobe axis to parallel laminated and normally graded in the channelized lobe off-axis areas. Similar facies changes have been observed along proximal to distal direction. The lateral change of the dominant structures in the beds indicates changes in the flow regime and depositional style.

Keywords: slope to basin floor, channel-to-lobe, facies, transition, Neuquen Basin, deep water basin margin, Los Molles Formation

Table of Contents

List of Tables

List of Figures

1. INTRODUCTION

Many studies have focused on deep water depositional systems due to the extensive growth of the industry interest in deep water petroleum plays (Galloway, 1998; Abreu et al., 2003; Posamentier, 2003; Mulder and Etienne, 2010) and with new data surfacing from technology advancement (Mohrig et al., 1999; Wynn et al. 2002; Olariu et al., 2008, 2011). In order to better understand the heterogeneity and geometric variability of the turbidite reservoirs there is often reliance on geostatistical modeling using subsurface data (well logs and seismic profiles) (Pyrcz et al., 2005, 2014). Modeling subsurface data without a good outcrop analogue can be difficult and inconsistent, thus there is a need to analyze sedimentary basins that offer good resolution, deep water outcrop analogues. In this study a 10 km long outcrop belt of slope and basin-floor deposits is analyzed and the objective is a better understanding of facies variability in the channelized to non-channelized (channel-lobe) transition.

It has been proposed that the transition between slope channels and lobes begins at the toe of slope where turbidity currents experience a hydraulic jump during transformation from confined to unconfined flow (Komar, 1971). Recognizing the channel-to-lobe transition zone is an important, but a commonly disregarded element of many deep-waters systems, sometimes because of the quality and resolution of the acquired data (Wynn et al., 2002). The transition zone has been recognized in outcrops (Mutti and Normark, 1991) and in the modern deep water settings (Palanques et al, 1995) as being composed of amalgamated sandstones, increased occurrence of scouring and bypass indicators linked up-dip with canyons and down-dip with sandy lobes (Wynn et al., 2002).

In the modern Valencia Fan differentiations have been made between three zones within a slope to basin floor evolution (Fig. 1), the channelized, transitional and depositional areas using sidescan sonar and shallow seismic (Palanques et al, 1995, Wynn et al., 2002). Offshore Morocco and Portugal in modern Agadir and Lisbon fans, at the base of the slope, the transitional zone between channelized and depositional deposits has been recognized to cover an area ranging from 40-60 km in length with the largest erosional features (scours) occurring with the change in gradient (Wynn et al., 2002). Downdip of the transition zone deposition is expected to occur in the form of lobes, which have been considered to be the corresponding distal part of a channel-levee system, describing non-channelized sand bodies (Mutti and Ricci Lucchi, 1972). Despite morphological models based on modern data or conceptual models based on vertical successions (Prelat et al., 2009, 2013, Burgreen and Graham, 2014) there is limited data on the facies variability in the channelized to lobe transition zone, making it difficult to follow continuous deposits laterally (Brunt et al., 2013),

The purpose of this study is to describe and interpret the down-fan evolution of sediment gravity flow deposits, with emphasis on the facies and architecture changes that occur at the transition from channels to lobes of the Jurassic Los Molles Formation in Neuquen Basin. The continuous outcrops permit a sub-regional correlation of the shallow water (shelf to shelf edge) to deep water (slope and basin floor) deposits. Using measured sections, large photo-panels and satellite imagery, this thesis focuses on changes that occur within the same deep water lobe beginning with the toe of slope and continuing onto the basin floor. This study presents quantitative data and proposes a model that can help predict architectural and facies changes within a deep water depositional environment at the channel-to-lobe transition zone based on detailed description of two lobe units.

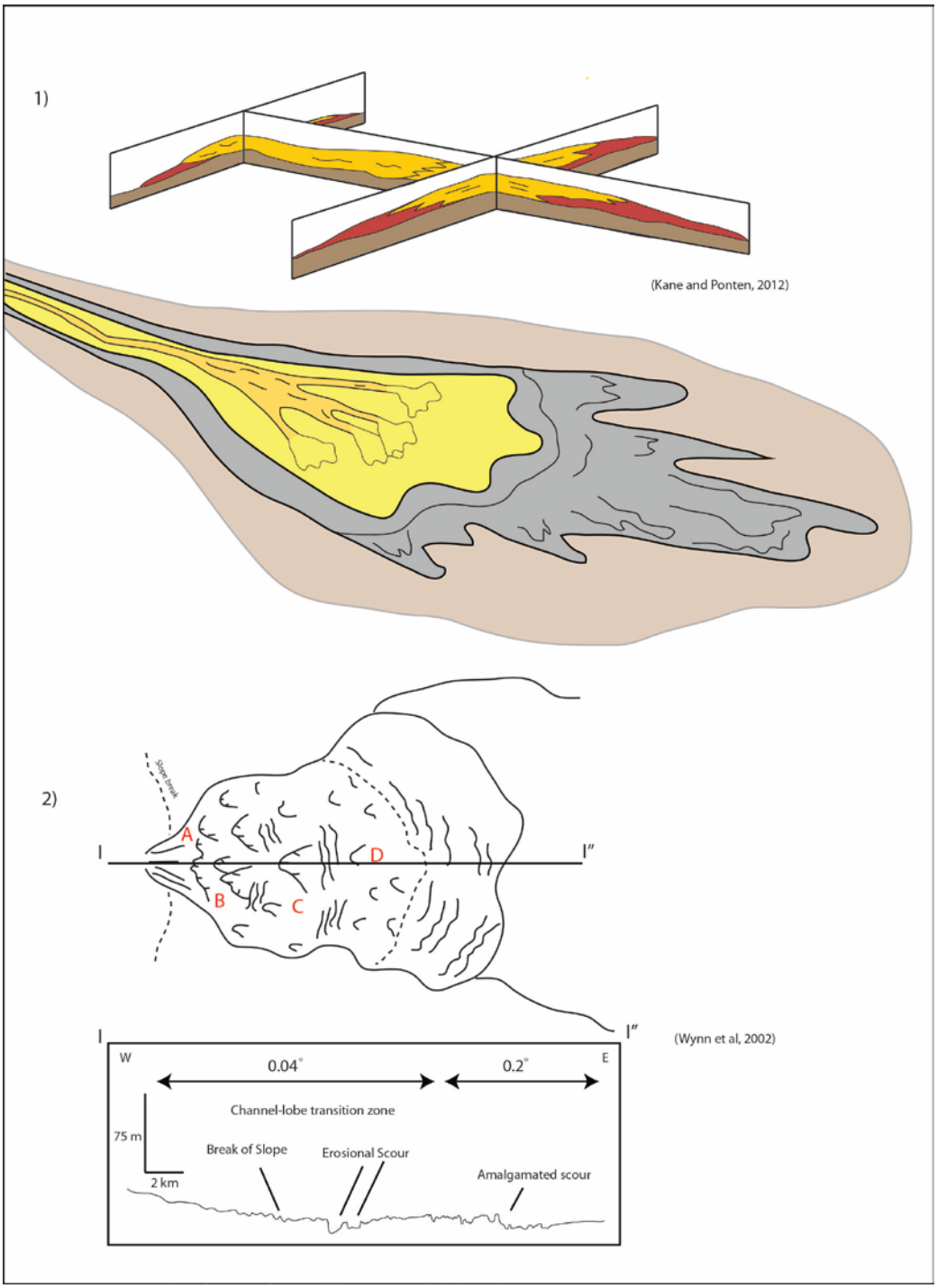

Figure 1 Previous work showing models for transitions within the deep water systems based on cores or modern environments (Wynn et al, 2002; Kane and Ponten, 2012)

2. GEOLOGIC SETTING

2.1 TECTONIC FRAMEWORK

The Neuquen Basin is triangular shaped, has 160,000 km² and extends up to 700 km in a north-south direction (Vergani et al., 1995). Neuquen Basin (Fig. 2) is a back-arc basin located along western-central Argentina (Paim et al., 2008), with a multiphase tectonic history that started with an initial extensional period during the Early Triassic remaining active until the Early Jurassic (Franzese et al., 2006). The basin records at least 200 My of subsidence with a 7000 m thick sedimentary succession ranging from Upper Triassic to Cenozoic (Vergani et al., 1995). The Mesozoic subsidence was linked with the thermo-mechanical collapse of a Late Paleozoic orogenic belt that fringed the southwestern margin of Gondwana (sensu Legarreta and Uliana, 1996). During the Toarcian-Aalenian to Bathonian-Callovian interval, the Neuquen basin underwent thermal subsidence, causing the expansion of the marine sedimentation in the basin (Franzese et al., 2003). Crustal thickening during the Late Early Permian and Late Permian uplift caused diffuse extension and multiple rift basins developed during Middle Triassic (sensu Legarreta and Uliana, 1996). Bounded in the northeastern by the Pampeano-Sierra Pintada Massif and the North Patagonian Massif (Somun Cura) in the southeast (Paim et al., 2008), a series of fault-controlled depocenters formed due to the development of half grabens oriented differently throughout the basin (Franzese et al., 2006).

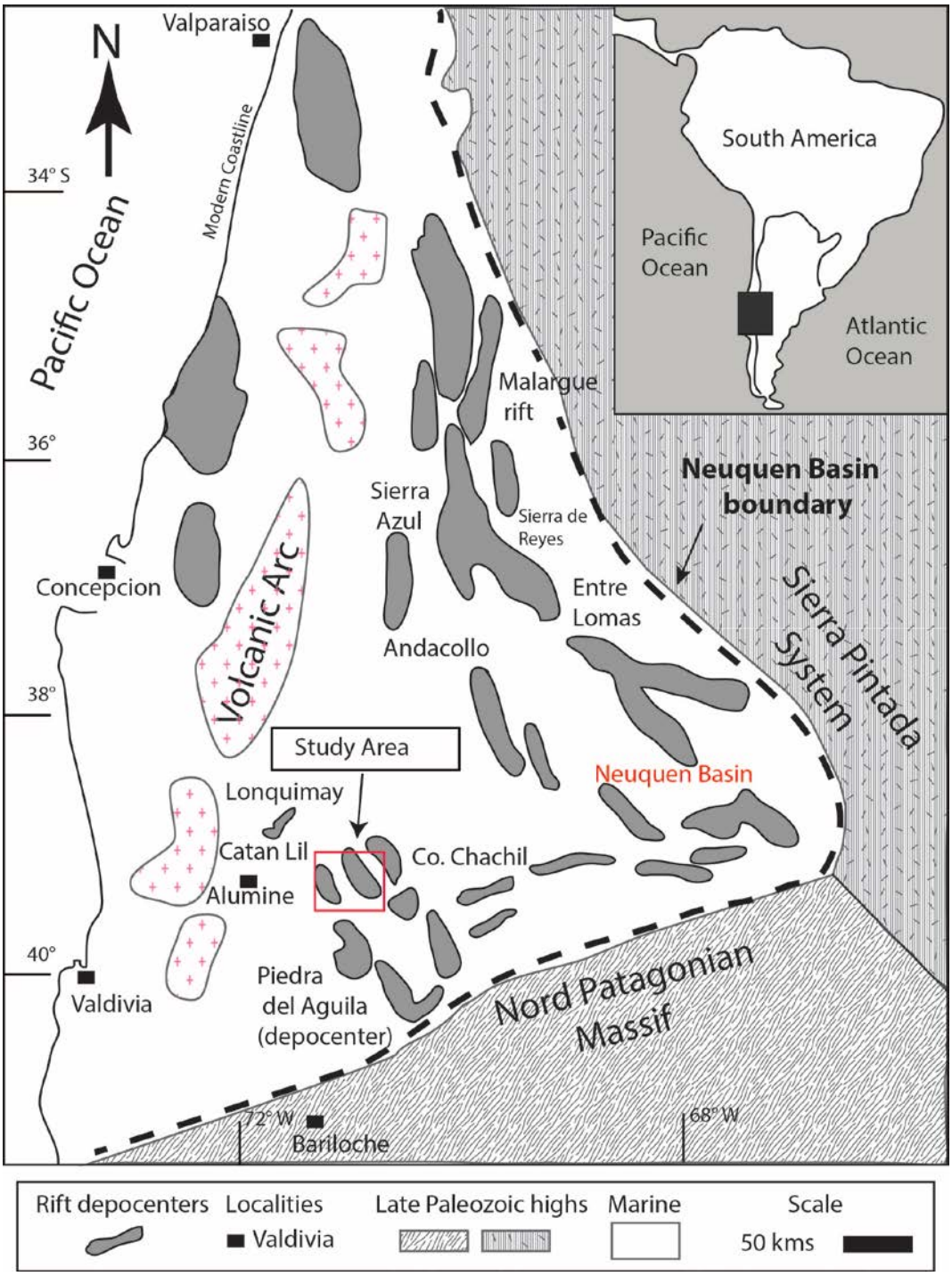

Figure 2 Location map for study area in the southern part of Neuquen Basin, central-west Argentina, with rift depocenter distribution and the adjacent highs (North Patagonian Massif and Sierra Pintada Massif). Study area is La Jardinera area near Fortin 1° de Mayo (modified after Franzese et al., 2006).

The initial infill of the syn-rift sediments is known as the Pre-Cuyo Group and the lowest Cuyo Group (Franzese et al., 2006). The synrift strata is made up of mostly siliciclastic sediments which were deposited in alluvial fan, fluvial, and lacustrine environments with significant pyroclastic deposits (Grimaldi and Dorobek, 2011). The tectonic activity waned during a post-rift period, with increased subsidence associated with a thermal sag stage (Vergani et al., 1995). It was during this time there was the first large invasion of marine water. Cycles of transgressive-regressive deposits also known as the Cuyo Group (Grimaldi and Dorobek, 2011; Vergani et al., 1995), were deposited as a consequence of an established connection with the paleo-Pacific Ocean. The post-rift period lasted until the Late Cretaceous when the area transitioned into a retro-arc foreland basin (Grimaldi and Dorobek, 2011). The isolated rift depocenters of early Jurassic gradually merged into a larger basin and the previous inter-basin highs had less of an influence (Vergani et al., 1995). The basin experienced numerous inversion periods, with the most important being responsible for the development of the Huincul Arch, a large east-west transcurrent fault zone, related with the extensional stresses caused by the Gondwana break-up and the Atlantic ocean opening (Vergani et al., 1995). The Huincul Arch divided the basin into two depocenters known as the northern and southern sub-basins (Grimaldi and Dorobek, 2011). The basin developed as a foreland depocenter during Late Cretaceous to Cenozoic times (Vergani et al., 1995, Franzese and Spaletti, 2001, Naipauer et al., 2012), with numerous inversion periods affecting the basin.

The sediment sourcing in the study area was from the south-southwest from the North Patagonian Massif (Somun Cura), a late Paleozoic metamorphic terrane part of the Patagonian platform, with possible granitoid units creating a northern outer rim (Ramos, 2008). Sediment

may also have been sourced from an immature volcaniclastic source in the west, an island arc system, suggesting a mixed provenance (Burgess et al., 2000).

The present study area is located east of the Alumine River and has been affected by the tectonic development of the southern Neuquen Precordillera (west verging fold and thrust belt) (Morabito et al., 2012). In the same area, later inversions of the N-NW orientated normal faults (e.g. Rahue fault) have been described. These created a W-NW verging syncline and anticline (Fig. 3), part of a fault-propagation fold formed through contraction which brought Jurassic strata to the surface. Great exposures of basement units, syn-rift and post-rift sedimentary deposits of Neuquen Basin were thus created. In Miocene times, magmatic activity occurred along reverse faults and established the present day topography in the study area (Morabito et al., 2012).

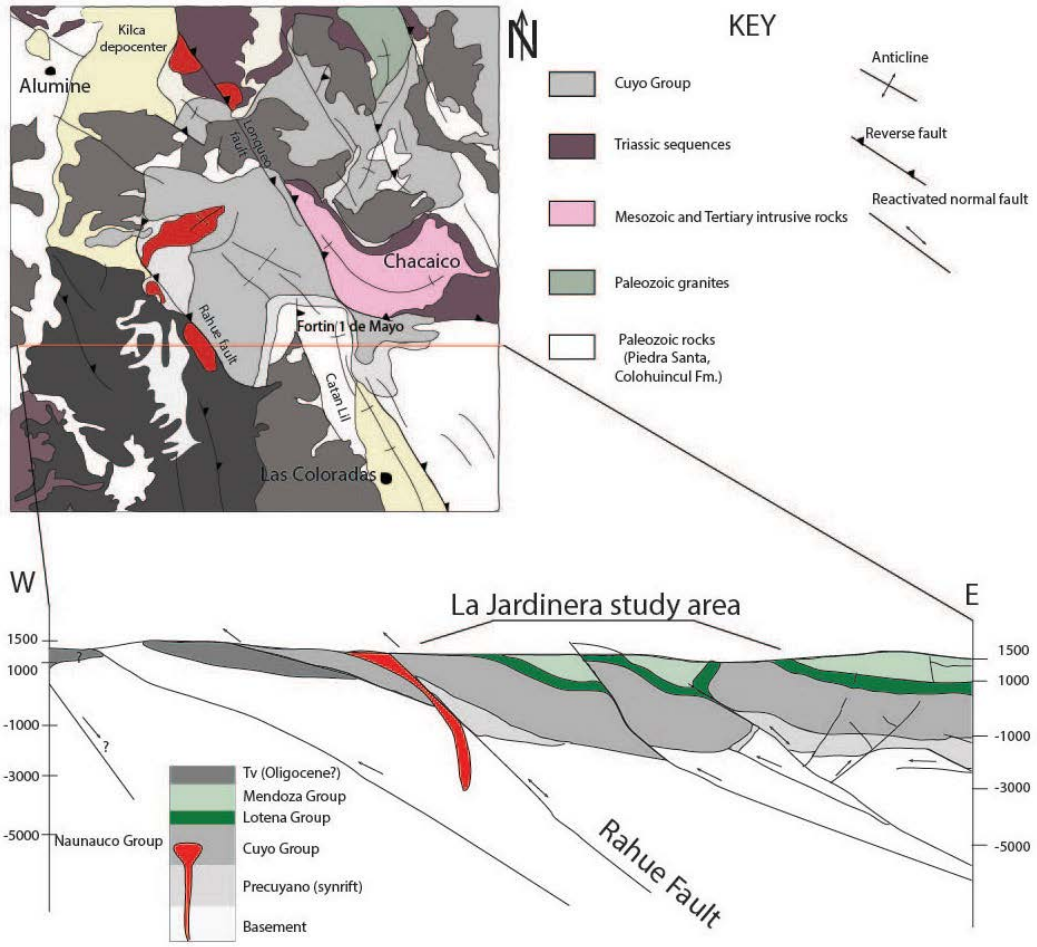

Figure 3 Geologic map and cross-section of the study area, La Jardinera, showing reactivated Triassic normal faults. , These are east verging, thrusting the Jurassic deposits to the surface, forming a NW verging anticline and syncline (modified after Morabito et al., 2012).

2.2 STRATIGRAPHIC FRAMEWORK

The basement consists of igneous-metamorphic rocks, low grade Silurian-Devonian schists and phyllites of Piedra Santa Formation, intruded by late Paleozoic granitoids, Chachil Plutonic Complex (Fig. 4). The Pre-Cuyo Group deposits are known as the Lapa Formation and consist mostly of lava flows, pyroclastic successions and siliciclastic continental sedimentary rocks (Muravchik et al., 2011). The first marine sediments, Cuyo Group, comprise of about

2,000 m of deposits that began accumulating during Hettangian-Pliensbachian with the deposition of the Sierra de Chacaico Formation, comprised of littoral to neritic sandstone and mudstones, followed by a deepening of the basin, with the deep water marine deposits, dark shale and sand-rich basin floor known as the Los Molles Formation (1000 m thick). Los Molles is, in turn, overlain by sand-rich shallow marine deposits of the Las Lajas Formation (600 m thick), (Zavala, 1996). In the study area of La Jardinera (Figs. 2, and 5) the fluvial component of the source-to-sink system, the Challaco Formation (Paim et al., 2008), is also recognized. Challaco Formation was not studied during this project, but its stratigraphic boundaries were approximately defined. The deep marine strata of the Los Molles Formation are predominantly gray and black mudstones, siltstones and sandstones related to “turbidite lobes” (Gulisano and Gutierrez-Pleimling, 1994; Burgess et al., 2000; Paim et al., 2008). The geochemical characterization shows that the Los Molles Fm. probably accumulated in isolated depocenters both in marine (south) and lacustrine (north) settings (Martinez et al., 2008).

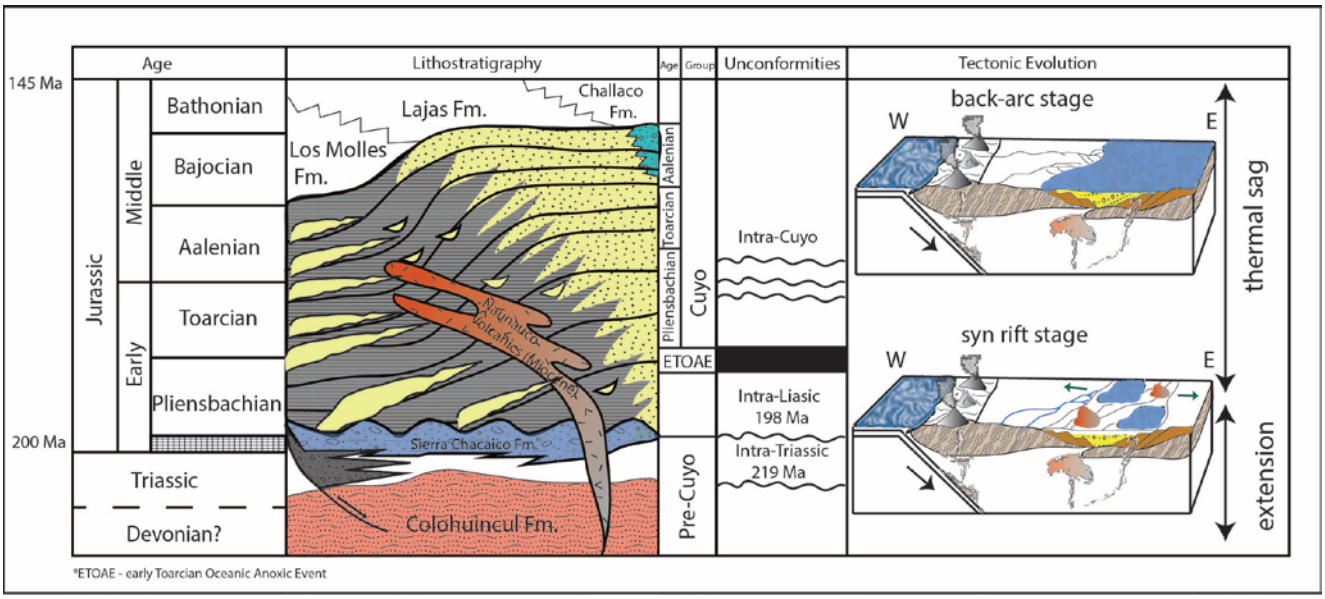

Figure 4 Stratigraphic framework for Los Molles Formation in the Southern part of Neuquen basin (Vergani et al., 1995; Riccardi et al., 2000,; Morgans-Bell et al., 2005; Paim et al., 2008; Kochann et al., 2011)

The suggested age for the Los Molles Fm. in the central-western part of Neuquen is late Aalenian to Bajocian (Martinez et al., 2008). In the study by Riccardi et al., (2000), the occurrence of characteristic ammonites, bivalves, brachiopods and calcareous microfossils extended the age of the Los Molles Fm. as early as Pliensbachian. Radiolarian fauna was described mid-section in the La Jardinera area, revealing a possible Toarcian-Aalenian boundary, (Kochann et al., 2011). Wood fragments, found in the Las Lajas Fm., in the La Jardinera area suggest ages ranging all the way to Early Bajocian (Morgans-Bell et al., 2005).

3. DATA AND METHODOLOGY

The focus for this study was around the La Jardinera Arroyo, a 200 km² area, located in the southern part of the basin, on National Route 46 (Fig. 5). Excellent (kilometers wide and hundreds meter thick) oblique to down-dip outcrop belt correlates with along strike outcrops, giving the opportunity to observe clinoform development of an Early-Middle Jurassic source-to-sink depositional environment in a back-arc basin. Fifty sedimentary logs (Fig. 5), approximately 4000 m of measured section allows 3-D architecture and geometry mapping of slope and basin floor deposits in a down-dip profile south to north for approximately 6 km and across-strike profile for approximately 3.5 km west to east orientation. High resolution (0.5 m) satellite image and a Digital Elevation Model (1m vertical resolution) were acquired and used to map out and digitize 8 different sandstone units (interpreted as deep water lobes) across the study area, using regional correlated mudstone intervals in-between. Two main sandstone units (Unit 6 and Unit 7) were mapped on the ground by walking and analyzed in detail (facies, grain size, bed thickness). Paleoflow measurements are scarce with just 26 paleocurrents measurements throughout the study area showing a NE dominance for the flow direction; rare W-E currents appear in thin heterolithic beds where tool marks or ripples have been used. Highly detailed (cm scale for km long outcrops) photomosaics (Gigapans), have been collected and used to identify architectural geometries and boundaries between sandstone intervals across the region. Small offset reverse and normal faults (meter to decimeter scale) affect the area but not enough to significantly disturb the stratigraphic correlation. The lateral continuity in unconfined channels was defined based on the width: depth aspect ratio, measured perpendicular to flow/paleoflow direction (Clark and Pickering, 1996).

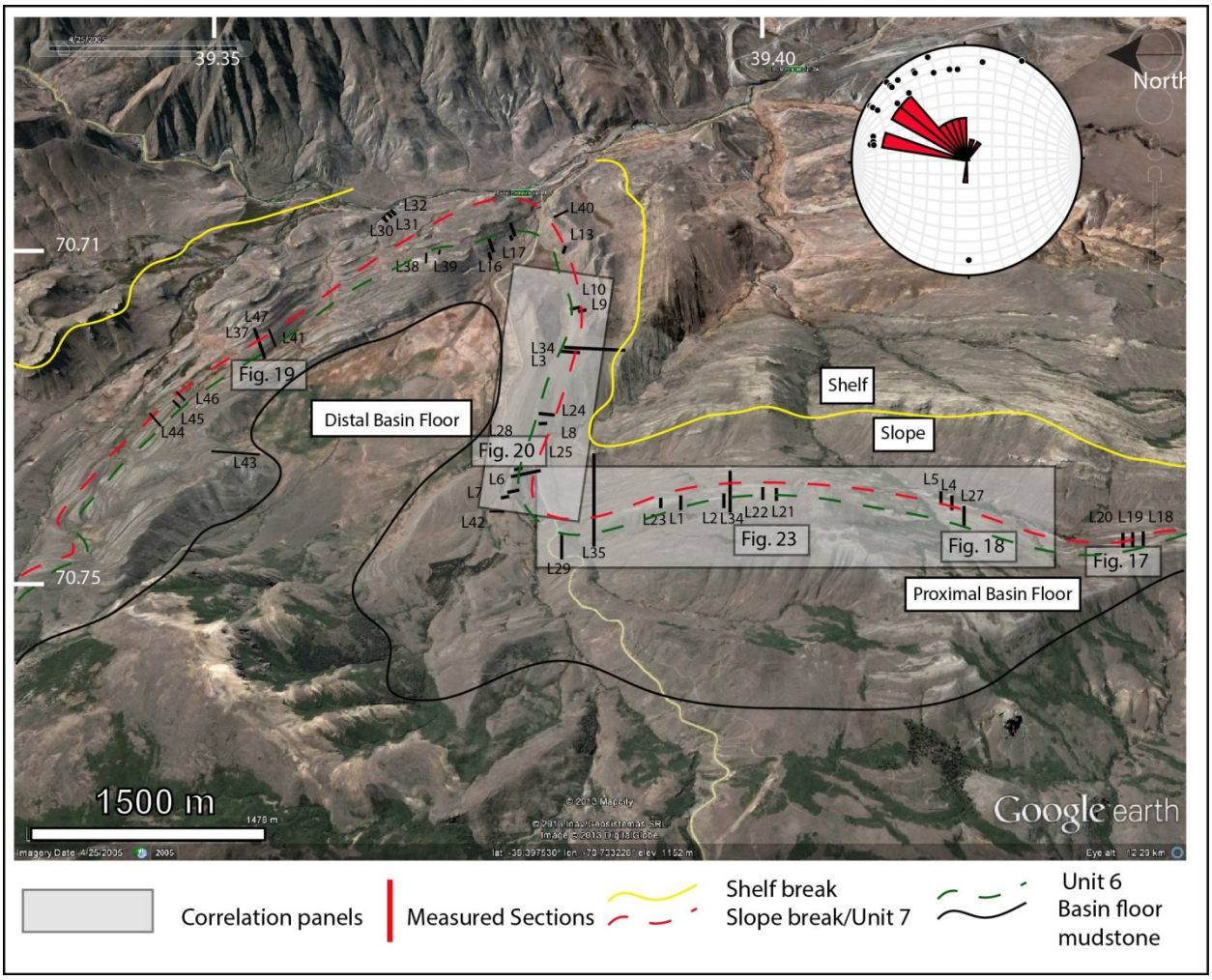

Figure 5 Google Earth satellite image showing location of correlation panels, measured sections and other figures within this study in La Jardinera area.

Lateral correlation of the units was made on satellite image and photo-pannels. Bed thickness, grain size and facies were used to map variability in units (lobes) 6 and 7 along dip and strike directions and in 3-D (map). Matlab software has been used to quantify and compare the data from the measured sections (Fig. 6). Firstly, we use scripts to extract grain size and bed

thickness distributions from drafted measured sections and we plot the data into histograms (e.g. normally or lognormally distributed). Secondly, scripts were used to read the facies interpretations for any given unit within the drafted measured sections, resulting in a variety of percentages which we plot into an area graph along a given profile. The data (grain size, bed thickness, facies at each location) was imported into ArcGis and contour maps were created for net to gross sand ratios, facies, grain size or bed thicknesses (Fig. 6). The geological map of the studied area (Fig. 7) was reconstructed based on previous maps (Morabito et al., 2012; Paim et al., 2008) and previous field mapping seasons (Vann, 2013).

Lobes were differentiated in outcrops based on presence of the shale intervals, the lateral continuity and geometry, and overall thickening or thinning upwards patterns; the upper boundary of a lobe was assigned where the highest shale content of a given interval was visible. Lobes were recognized in a locally defined area, with smaller muddy intervals between the thicker lobe packages. Channels were recognized based on discontinuity in geometry, erosional relief along their bases, and thinning upward pattern or amalgamated pattern.

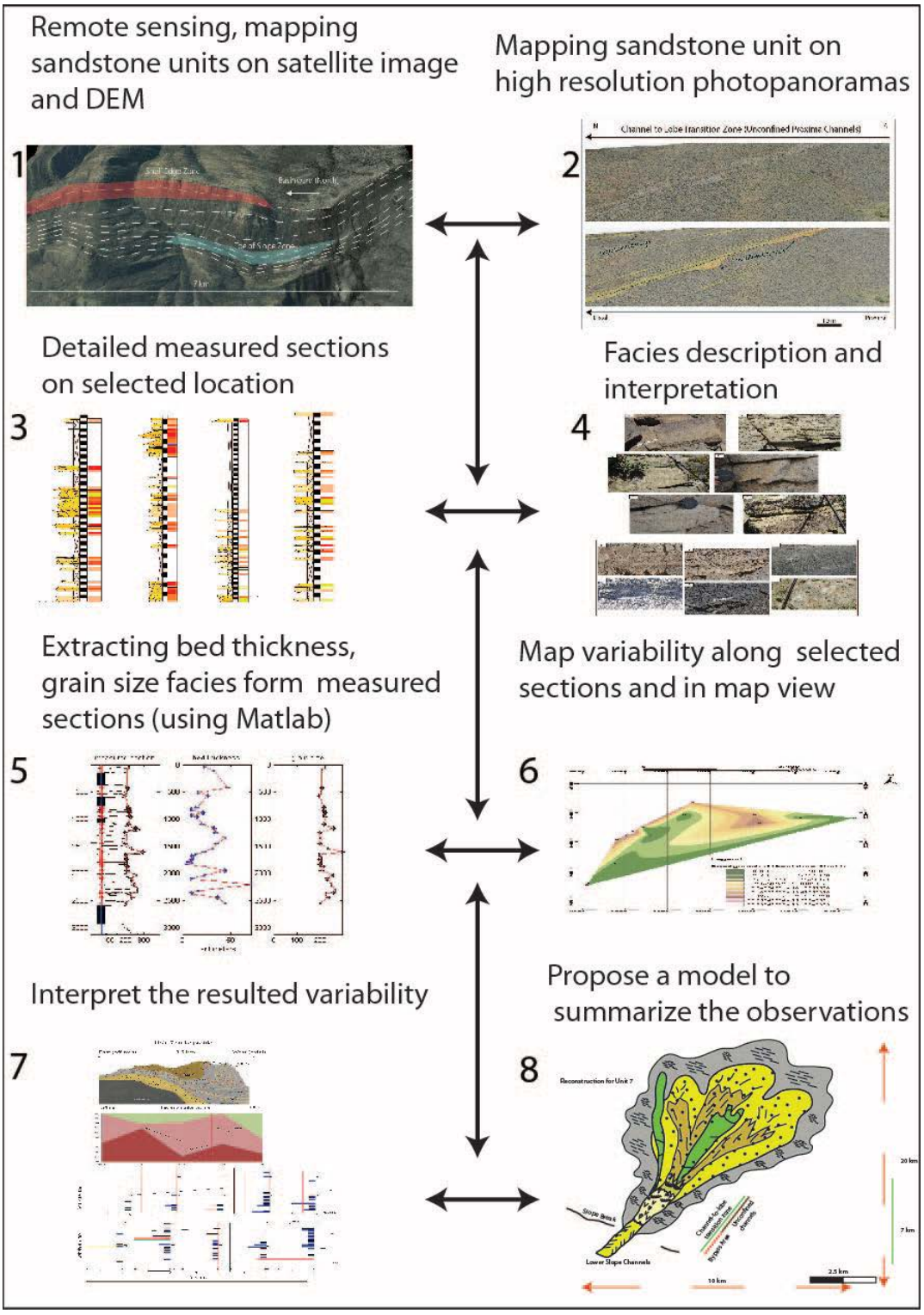

Figure 6 Methodology followed in this study from acquisition, processing and interpretation of the data

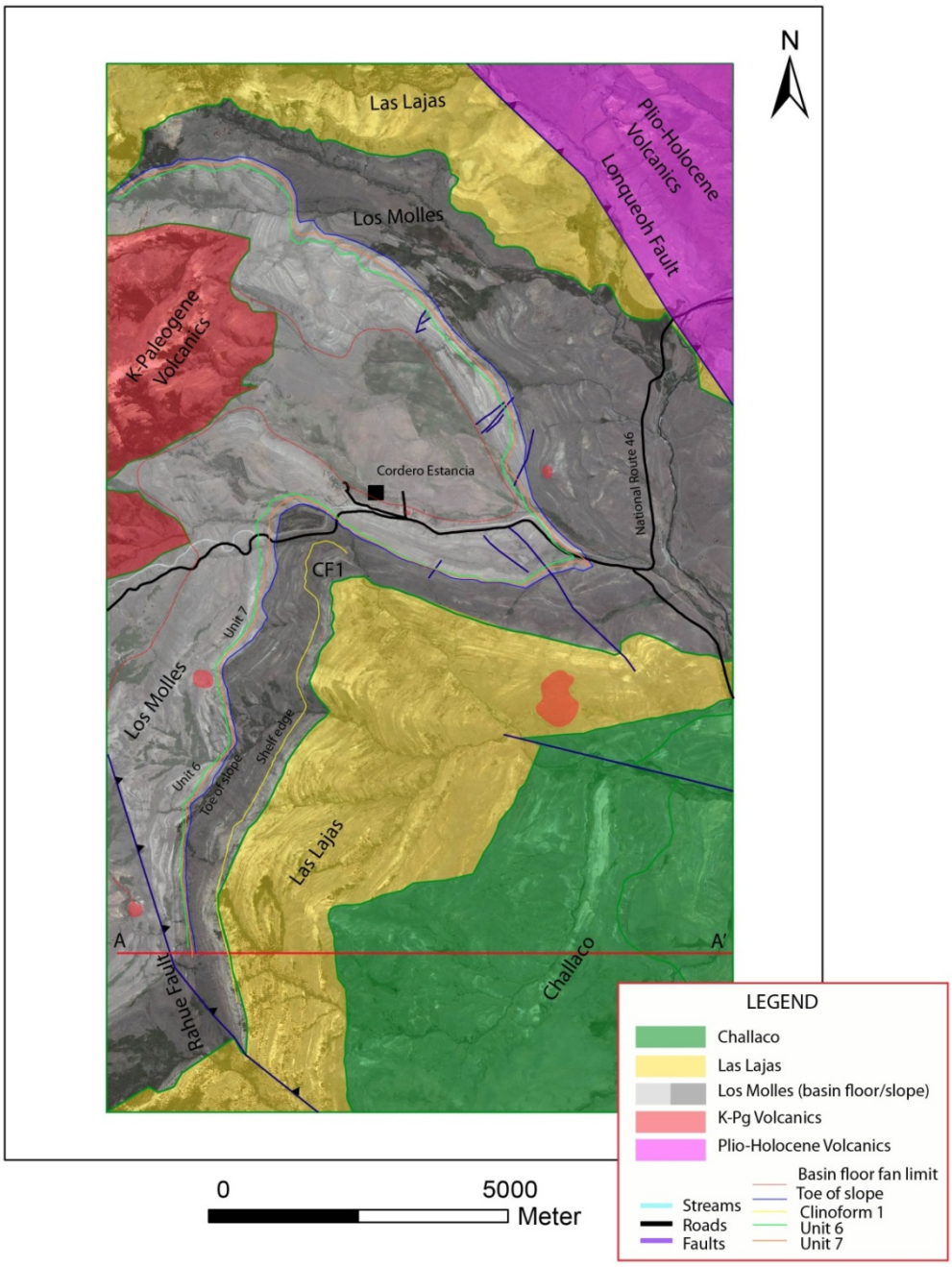

Figure 7 Geologic map constructed here but partly based on previous data (Paim et al., 2008, Morabito et al., 2012, Vann, 2013)

4. RESULTS

The La Jardinera outcrops (Figs. 5, 7 and 8) present a shelf to slope transitional area between the Las Lajas (shelf) and Los Molles (slope) formations, with a minimum run out slope length ~ 6-7 km, a shelf margin that prograded from S-SW to N-NE with a slope angle of ~ 1.6-3.8° (Vann, 2013). The shelf to basin floor system is coarse grained with thick conglomerates at the shelf edge area and conglomerate lenses or thin beds on the slope and occasionally on the basin floor (Paim et al., 2008, Vann, 2013). The average paleocurrent direction measurements (n=26) show a paleoflow orientated towards the N-NE (34°-65°) which is consistent with previous paleoflow measurements in the area (Paim et al., 2008; Vann, 2013). In the study area two deep water sandstone complexes interpreted as fans are separated by a thick muddy interval defined as inter-fan deposits (Fig. 8). Each of the fans has multiple (8-9) sandstone-dominated sub-units (lobes) with individual thicknesses between 5 to 15 m. The results discussed here focus on the architecture variability of two of these sandstone units, lobes 6 and 7 of the upper fan (Figs. 5, 8 and 11). The lobe units 6 and 7 as counted from the base of the upper fan were chosen because of their very good exposure and lateral continuity (Fig. 5).

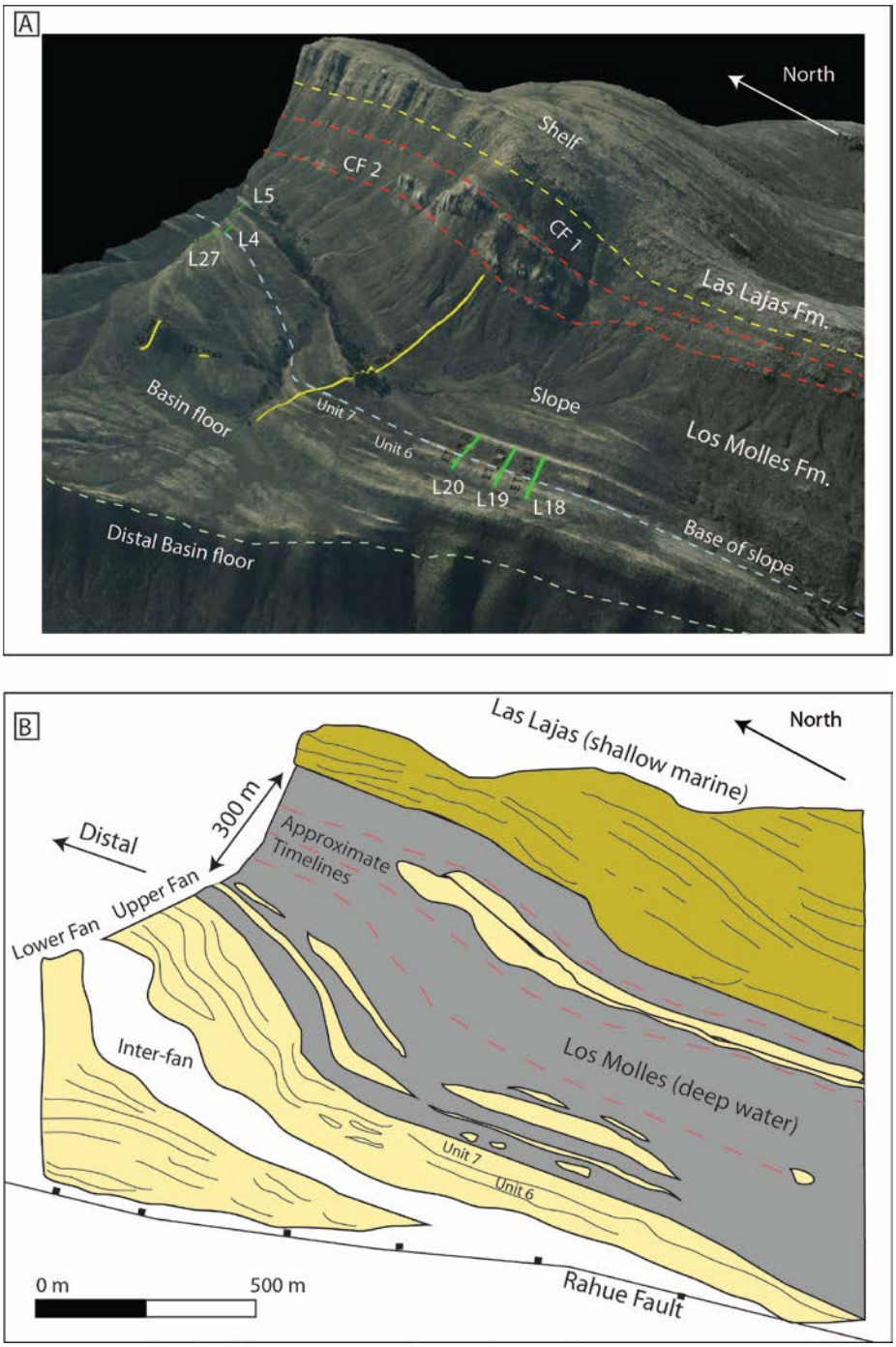

Figure 8 Architecture for the Los Molles Formation showing a vertical and lateral transition from shelf to basin floor, at Beymalek Estancia (A. Global Mapper 3D DEM with timelines and transitional boundaries between described environments in La Jardinera area, B. Interpretation of the different environments found in the study area based on measured sections and photo-panoramas)

4.1 Facies and Facies Associations of Los Molles Formation

The sedimentary facies concept continues to be a basic one in clastic sedimentology (Walker and James, 1992; Steel and Milliken, 2013), although an increase in the usage of detailed modern process analogues (Nittrouer et al., 2012; Shaw et al., 2013), has greatly boosted our knowledge and ongoing understanding of the variability of facies models. The main facies assemblages here were defined based on bedding style, sedimentary structures (physical and biological), fabric, and grain size. Eight representative facies have been recognized (Table 1 and 2, Fig. 9) in this study: a) mud-clast "rich" conglomerate (FA1), b) sand/pebble conglomerate (FA2, FA3, FA4), c) structureless sandstone, amalgamated and non-amalgamated, (FB1 and FB2), d) normally/reverse graded sandstone (FC1 and FC2), e) plane parallel/low angle parallel/cross-bedded sandstone (FD1, FD2, FD3), f) deformed deposits (FE), g) heterolithic interbedded sandstone and mudstone (FF), h) silty mudstone (FH). Paleoflow has been identified using measurements on flute/groove casts and tool marks, climbing ripples and low-angle cross bedding.

Deep water environments have undergone a range of classifications from Middleton and Hampton (1973) who separated deep water gravity flows into different flow types: debris flow, grain flow, fluidized-liquefied flow and turbidity current; Mulder and Alexander (2001) who divided subaqueous density flows into cohesive flows (debris flows and mud flows based on grain size distribution) and frictional flows (hyperconcentrated density flows, concentrated density flows and turbidity flows). New studies in the last decade have focused on co-genetic sandy and muddy sediment gravity flows, initially named linked-debrites (Haughton et al., 2003;

Jackson et al., 2013) later called hybrid-flows (Haughton et al., 2009) and more recently transitional flows (Sumner et al., 2009; Kane and Ponten, 2012).

As described by many authors (Haughton et al., 2003, 2009; Talling et al., 2007; Ito, 2008; Kane and Ponten, 2012; Jackson et al., 2013) sediment gravity flows undergo changes as they transport sediment down dip into the fan, changing over a run out length (Haughton et al., 2003) from turbulent into laminar (cohesive or non-cohesive) flows or vice versa. A flow which starts as a debris flow on the upper part of the slope and that partially transforms into a dilute turbulent flow that outruns the primary debris flow is called a hybrid-flow (Haughton et al., 2003; Talling et al., 2007). In this study, the focus was not on single bed flow transformation and their deposits but rather on the variability at a sub-regional scale of sediment gravity-flow facies and facies associations (grouped sedimentary facies that characterize a depositional environment).

Facies	Description	Interpretation	Depositional Environment
Mud rip-up intraclast conglomerate (FA1)	Clean sand to poorly sorted muddy matrix, 10 cm -20 cm thick, erosive/irregular contact, continous	Deposition from basal scouring turbidity current (Grundveg), clean and sand debris flow (Talling) high energy, erosive	Upper and lower slope channel lag, high energy channel axis
Mud/Sand to pebble conglomerate a) muddy/ poorly sorted (FA2) b)pebble conglomerate (FA3) c) sandstone clast conglomerate (FA4) well sorted	Mud/Sand to pebble conglomerate a) muddy matrix, cobble and rafted blocks, 10 cm to 2 m thick b) sandy matrix, well sorted 10cm to 1m thick c) sandy matrix, poorly sorted 10 cm - 30 cm	a) cohesive debris flow b) non-cohesive debris flow c) non-cohesive debris flow	a) slope and basin floor b) basin floor lobe c) channel axis/ fringe
Structureless Sandstone a) non-amalgamated (FB1) b) amalgamated (FB2)	Structurless sandstone, clean to poorly sorted, very coarse to fine grained, tool marks, sharp to erosive bases and sharp tops, 30 cm-50 cm, 2-3 meters during amalgamation	High-density turbidity currents with depletive steady and unsteady flows	Basin floor lobes and slope channels, increasing amalgamation indicating flow axis and degree of proximity to confinement
Normally/Reverse Graded Sandstone (FC1, FC2)	Normal graded sandstone, very coarse/pebble to medium/fine sand, with occasional, sharp to erosive bases, local scour and fill, sole marks and rare burrows, rare plant fragments occur, 20 cmto 1 m in thickness	High-density turbidity currents with depletive flows dominating	Slope channel axis, proximal and axial basin floor lobes

Table 1 Facies table showing the 9 different facies found and described in the La Jardinera area within the Los Molles Formation (1)

Facies	Description	Interpretation	Depositional Environment
Plane parallel, low angle parallel, cross bedded sandstone (FD1, FD2, FD3)	Coarse to fine sand, often faint plane parallel to cross-beds, wedge shaped, discontinous along a single bed, 10 to 50 cm thick, commonly overlying structureless or normally graded bed	Waning low density turbidity currents, high to low concentration flows, dilute turbidity current forms coarser grained upper plane bed regime, higher density form by en masse freezing or traction carpets	Basin floor lobe, lower slope channel
Deformed Deposits (FE)	Heterolithic sandstone and mudstone, 1-10 cm thick, mixed and amalgamated mudstone and fine to medium sandstone	Soft sediment deformation	Slope and Base of Slope
Heterolithic, interbedded, sandstone and mudstone (FF1)	Mud to silt interbedded with 1-10 cm , fine to coarse sand, up to 10 m thick packages, commonly sharp bases and drag marks on sand, sharp to fining up top, lenticular sand bodies, slump features common	Alternating suspension fallout deposits and low density turbidity current	Distal/off-axis basin floor lobes
Silty mudstone (FF2)	Dark, organic rich, mud with faint parallel laminations to structureless, slump features, commonly occuring in thick packages between sand layers, 1 cm to 5 m thick	Suspension fallout, background sedimentation	Distal/off-axis basin floor lobe, sedimentation during avulsion, slope

Table 1 Facies table continued

4.1.1. Facies A: Sand/pebble conglomerates (debrites) and mud-clast conglomerates

Description

This conglomerate facies was divided into four different sub-categories: A1) sandy conglomerate beds 10-20cm thick with disorganized texture, (with 5-10cm clasts)., Beds are poorly sorted, and ungraded (Fig. 9.1); A2) sharp-based conglomerate beds 10-50cm thick with a muddy matrix, and dominated by mud clasts distributed randomly with rare extra-formational pebbles/cobbles and no distinctive grading (Fig. 9.2); A3) beds of poorly sorted pebble conglomerate, 50cm to 1m thick, with cm scale well rounded metamorphic and volcanic clasts. They are also generally ungraded and have an irregular base (Fig. 9.3); A4) moderately sorted, erosionally-based pebble conglomerate beds, 20cm to 1m thick, often with "pencil-like" mud-clasts orientated parallel to the base (Fig. 9.4); The conglomerate facies A3 and A4 occur locally in the area, usually overlying a sandstone unit or being over- or under-lain by a thick mudstone interval.

Interpretation

Facies A1 (mud-clast rich structureless sandstone) is usually found at the base of channelized units, being a key indicator of strong erosion (upstream of that location) and bypass. The facies A1 is interpreted as the base (structureless) of a turbidite deposit. Based on the lack of internal sedimentary structures, the presence of large clasts mixed with muddy matrix, facies A2 is interpreted as *en masse* settling deposit (Lowe, 1982; Talling et al., 2012) with no segregation of clasts, preserving the muddy flow thickness, creating the deposit through the *freezing* of the flow (sensu Talling et al., 2012). In the case of facies A3 (Fig. 9.3) the size of the clasts and the poor sorting (>5 % gravel, Mulder and Alexander, 2001) indicate that it was deposited as a result of a coarse-grained debris flow that transported large clasts (cm to dm) from the upper

slope/shelf region. Facies A4 (Fig. 9.4) is a transitional debrite formed from an initial turbulent flow which led to the incorporation of a large quantity of mud clasts and pebbles and which transformed down-dip into a debris flow (laminar flow), being sheared at the base, aligning the mud clasts parallel to the base of the deposit. Some similar bed textures have been described from Gardner et al. (2003). Debris flow deposits (facies A2 and A3) are the result of turbulence suppression (Mulder and Alexander, 2001), producing laminar flow, with occasional weak turbulence and grain mixing in the flow (Talling et al., 2012). Whenever a two layer flow, with a layer containing outsize clasts (up to 2m in length) moving above a relative high shear-stress layer, the clasts of the lower layer may be sheared, like in the case of facies A4, and will probably become progressively deformed in the plug itself (Clayton, 1994). Mud-clast conglomerates (facies A1) are interpreted to be basal parts of the deposits of high density turbidity currents a short distance downstream from an active erosional area of muddy substrate (Smith and Spalleti, 1995). Mud "rich" conglomerates (facies A2) can be classified based on their dominant matrix as either muddy debrites or sandy debrites, deposited by a flow that can be either laminar or weakly turbulent (Jackson et al, 2013). During the development of scouring flow, high density currents develop shear stress at the contact with the substrate, dislocating it (forming mud clasts as in A1 facies) and due to cyclic loading it may even promote liquefaction (Butler et al., 2006) which might generate deposits described latter as facies E or F.

4.1.2. Facies B: Structureless sandstone (amalgamated or non-amalgamated)

Description

Facies B averages 30cm thickness for non-amalgamated beds and 50cm thickness for amalgamated structureless sandstone beds. Beds are ungraded, with a sharp erosional base, and show loading and some dewatering features (Fig. 9A). Beds show occasional tool marks and flute casts (indicating NE paleoflow direction), and there is some rare lamination present towards the bed top, with occasional organic (wood) fragments. Mud rip-up clasts (1-5cm), moderately to well-rounded, are commonly found at the base of the beds, and are rarely found towards the top or throughout the bed. Sandstone beds with a large content in mud clasts were grouped as mud-clast conglomerates (Facies A1). Amalgamation of structureless beds can be observed where there are clear grain size breaks, or where small mud clasts (1-2cm) or "pockets" of coarser grained (very coarse to gravel) material concentrate (Fig. 9F). Convolute lamination and/or truncation of older, underlying beds (Fig. 9.6) may also occur in this facies.

Interpretation

The structureless sandstone beds are interpreted as high density gravity flows (Lowe, 1982, Talling et al., 2012) or concentrated density flows (Mulder and Alexander, 2001), probably connected with the axial fairway of the flow (Lowe, 1982). A rapid decrease in flow velocity results in abrupt fall-out of sediment, which suppresses development of tractional structures or sorting of grains at the base. Mud rip-up clasts at some locations suggest high density aggrading flows, forming possible in a depletive steady flow (Kneller and Branney, 1995). Mud-clasts are interpreted to have been derived from erosion of the muddy slope or basin floor by high or low density flows (see earlier discussion about mud clast conglomerate). The presence of mud-clasts at the top of the beds (Fig. 9.1) may occur because of increased differentiation of density within

the turbulent flow and/ or the incorporation of the clasts towards the end of the flow or transport as part of a laminar flow (for higher density concentrated flows) (Cartigny et al., 2013, Jackson et al., 2013).

4.1.3. Facies C (Normal and inverse-graded sandstone)

Description

Normally graded sandstone beds with a decreasing upward grain-size trend from coarse (occasional gravel) to fine sandstone to silt at the top are commonly 20cm to 1m thick (Fig. 9.7). In some beds an inverse grain size grading has been observed, especially near the base of the bed (Fig. 9.8). Beds are generally poorly sorted, with sharp to some locally erosive bases, coarse to gravel grain size "pockets" infilling local depressions in topography (Fig. 9F). Mud clasts (1-5cm diameter) are often present at the base of the normal graded bed. Normal graded beds have occasional basal flute casts and tool marks.

Interpretation

Beds with graded (normal or inverse) grain size are interpreted as density flows or turbidity currents where the grading is a function of pseudoplastic behavior of particle suspension in high concentration and through particle interaction (dispersive pressure) within the suspended sediment (Middleton, 1967; Lowe, 1982). In low-density turbidity currents, which are likely to be fully turbulent, turbulence becomes the main support mechanism for sediment (Lowe, 1982), overriding the hindering settling that affects high-density turbidity currents and reworking grains as bedload (Talling et al., 2012). The inverse grading indicates that the basal shear was high enough to generate dispersive pressure in the flow exerting an upward force on the larger particles (Clayton 1992).

4.1.4. Facies D (Parallel laminated and cross-stratified sandstone)

Description

This facies assemblage consists of 30-40cm thick fine to coarse-grained beds with parallel or low angle laminated sandstones (Fig. 9.10), sharp base (planar laminated) or erosional base (scour-and fill cross bedding), with rare gradation into silty beds at the top (Fig. 9.9)

Interpretation

The laminated (parallel or cross-stratified) sandstone facies represents deposits formed from low density turbidity currents in waning, high to low concentration flows. Dilute turbidity currents form coarser grained (upper medium or occasional coarse size sand) intervals in the upper plane bed regime, as a linked low density to higher density flow and which accumulates from *en masse freezing* or traction carpets (Talling et al., 2012). Planar and cross-lamination are related with bed load traction and sedimentation from low density turbidity currents (Bouma, 1968, Lowe, 1982, Talling et al., 2012).

4.1.5. Facies E (Slump)

Description

Facies E comprises heterolithic sandstone and mudstone in beds usually 1-10 cm thick, sometimes in excess of 1 m thick units., The sandstone component is fine to medium grained (Fig. 9.11) with sharp base. Deformation is common and is expressed as small scale overturned folds with a ductile component to the deformation (Fig. 9C); locally small reverse faults are present.

Interpretation

Facies E is interpreted as fine-grained, locally unstable slope deposits caused by high sedimentation rates, high pore pressure, and common oversteepening. Slumping, that generate meters thick deformed units, occurs whenever the downslope component of the shear stress induced by the weight of the sediment exceeds the sediment cohesion (Hesse, 1995). The soft-sediment deformed deposits are found associated with deep water channels or within lobe fringes, thick heterolithic sandstone and mudstone intervals, in low energy settings, or with reverse and normal faults, mostly chaotically deformed (see also Oliveira et al., 2011).

4.1.6. Facies F (heterolithic beds and silty mudstones)

Description

Facies F1 consists of interbedded mudstone and fine to medium-grained sandstone beds, the latter are commonly structureless, occasionally with rare planar laminations and climbing-ripples. The sandstone beds have sharp bases, with drag marks and flute casts (N-NE paleocurrent direction). Lenticular sandstone beds (cm thick and meters long) alternate with thin bedded normally graded coarse to fine grained sandstone. The thin bedded Facies F intervals form meter-scale packages (up to 10m) and are in many locations associated with slumping/sliding (Facies E). Thick mudstones (tens of meters) are found in the distal part of the fan. It is common to find body fossils ammonites, belemnites and bivalves, preserved within the mudstones.

Interpretation

The thick black mudstones (Fig. 9.12), which lack any sandstone intercalations of facies F1 are interpreted as a product of dilute turbidity currents which are found commonly in the distal part of the basin floor or as ‘turbidite mudstone’ (associated and transported within the flow that

created the underlying bed) (sensu Talling et al., 2004). The thin sandstone beds associated with the siltstones/mudstones were deposited in a frontal position of the main feeder or an off-axis/fringe area (sensu Lucchi et al., 1980), through alternating sediment suspension fallout and low to medium density turbidity currents. The current ripple cross-lamination associated with the thin sandstone beds indicates tractional processes and bedload transport during a low density turbidity flow event (Talling et al., 2012). A bed thickening-upward trend is present within many of the heterolithic intervals which may indicate an increase in the strength/volume of turbidity currents over time (Johnson et al., 2001).

Figure 9 full caption next page

Figure 9 Facies described and interpreted within the Los Molles Formation (1.Mud-clast conglomerate in lower slope channel, 2.Mud matrix debrite, 3. Pebble conglomerate, 4. “pencil-bed” pebble conglomerate, 5.Non-amalgamated structureless sandstone, 6. Amalgamated structureless sandstone, 7. Normally graded sandstone, 8. Reverse graded sandstone, 9. Planar laminated sandstone, 10.Cross-bedded lenticular sandstone, 11. Soft deformated beds (slump), 12. Mudstone interval) and the facies associations describing the different vertical and lateral relationships between the facies types (A. Mud-clast conglomerate capped top and bottom by high density structureless sandstone in the fringe of a lobe, B. Pebble conglomerate cuts into underlying structureless sandstone, C. Mud-clast conglomerate bounded by mudstone above and below , D. Muddy debrite overlying a high density structureless sandstone, E. Transition between “pencil-bed” pebble conglomerate and high density structureless sandstone, F. Normally graded sandstone eroding into underlying planar laminated sandstone)

4.2. DEEP WATER ARCHITECTURE OF LOS MOLLES FORMATION

The deep water architecture of the studied Los Molles Fm. was visible and imaged at the large scale using high resolution photo-panoramas and a satellite image draped over a Digital Elevation Model (Figs. 7 to 9). Large scale clinoforms that connect the shallow-water shelf deposits from the deepwater slope deposits have been recognized along S-SW to N-NE oriented outcrop transects. Basin margin clinoforms which separate dominantly shallow water from dominantly deep water deposits can form in any type of sedimentary basin that has enough depth (usually larger than 200 m) that allows the development of a shelf- slope break (Steel and Olsen, 2003). The shelf-slope break can be a subtle gradient change as little as 1 degree, but it can be identified at most deepwater margins except across shelf margins in their embryonic stages, in which cases it forms a shelf-slope ramp (Helland-Hansen et al., 2012). In the La Jardinera study area, Paim et al., (2008) described shelf, slope and basin floor deposits but did not identify the clinoforms. The separation of the depositional domains (shelf, slope and basin floor; Figs. 7, 8 and 11) was based on field mapping of the deposits, tracing on the DEM satellite image and

using some of the observations of Paim et al., (2008). In this study the basin floor deposits are separated into two fans, upper and lower, with an inter-fan muddy interval (Fig. 8). Each fan has at least 8 component sandstone units (lobes) each around 10-15 m thick. This study focusses on the upper fan and more explicitly within two lobes (units 6 and unit 7) of this upper fan, selected based on continuous outcrop exposure along the down dip and along strike profiles. The separation between the upper and lower fans was done through the recognition of a thick muddy interval (~ 100m) lying between two sandy dominated intervals across the region (Figs.7 and 8).

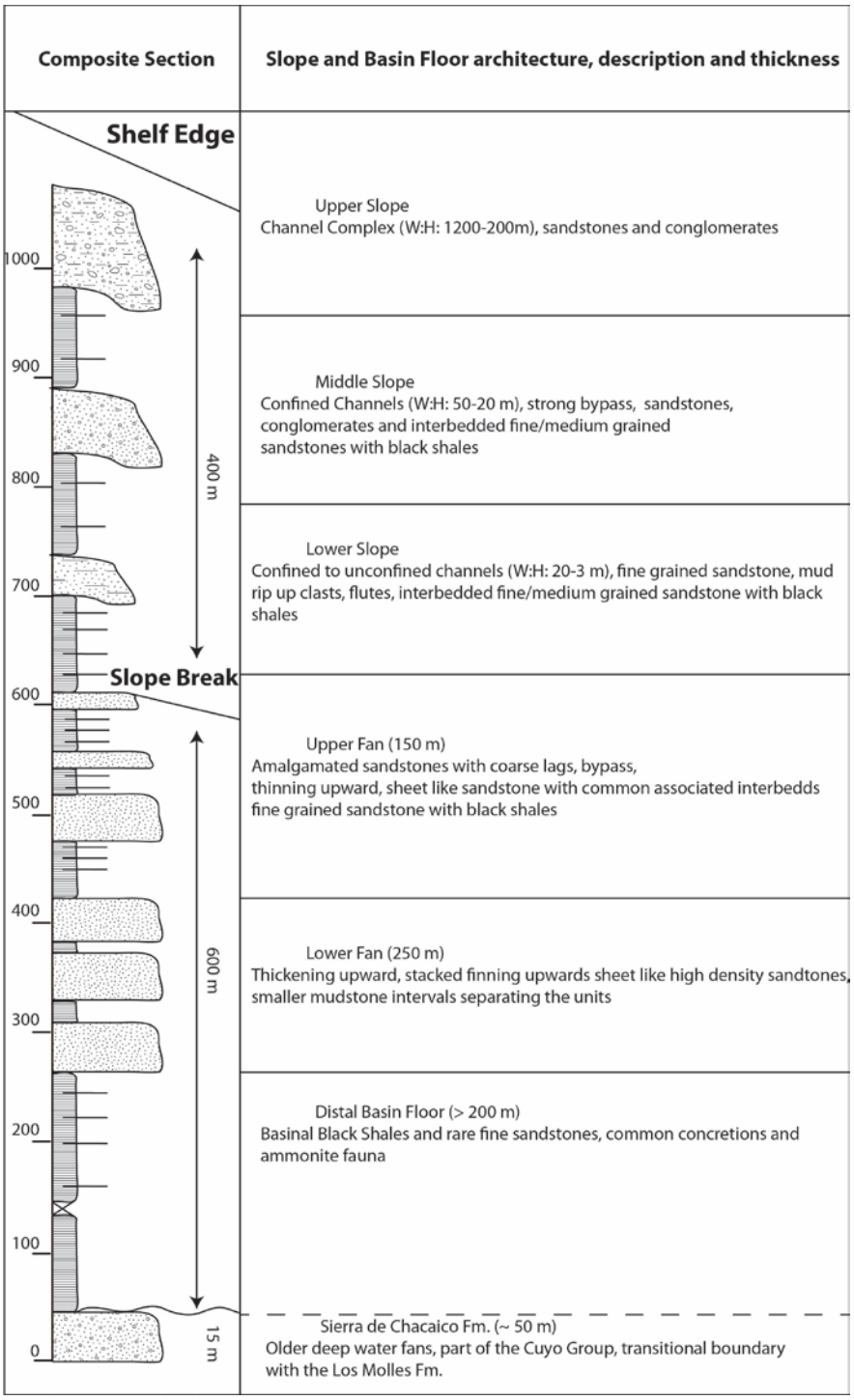

Figure 10 Composite section showing the thickness variation for the interpreted environments within the Los Molles Formation in La Jardinera area

Facies and architecture differences between large channel complexes, mid- to lower slope confined channels, proximal channelized lobes to middle fan lobes (Vann, 2013) have been recognized. However the focus is on transition from deep water channels to lobes. Channels are recognized based on their negative relief produced by confined gravity flows and are usually the result of bypass and a long period of sediment transport pathway (Johnson et al., 2001).

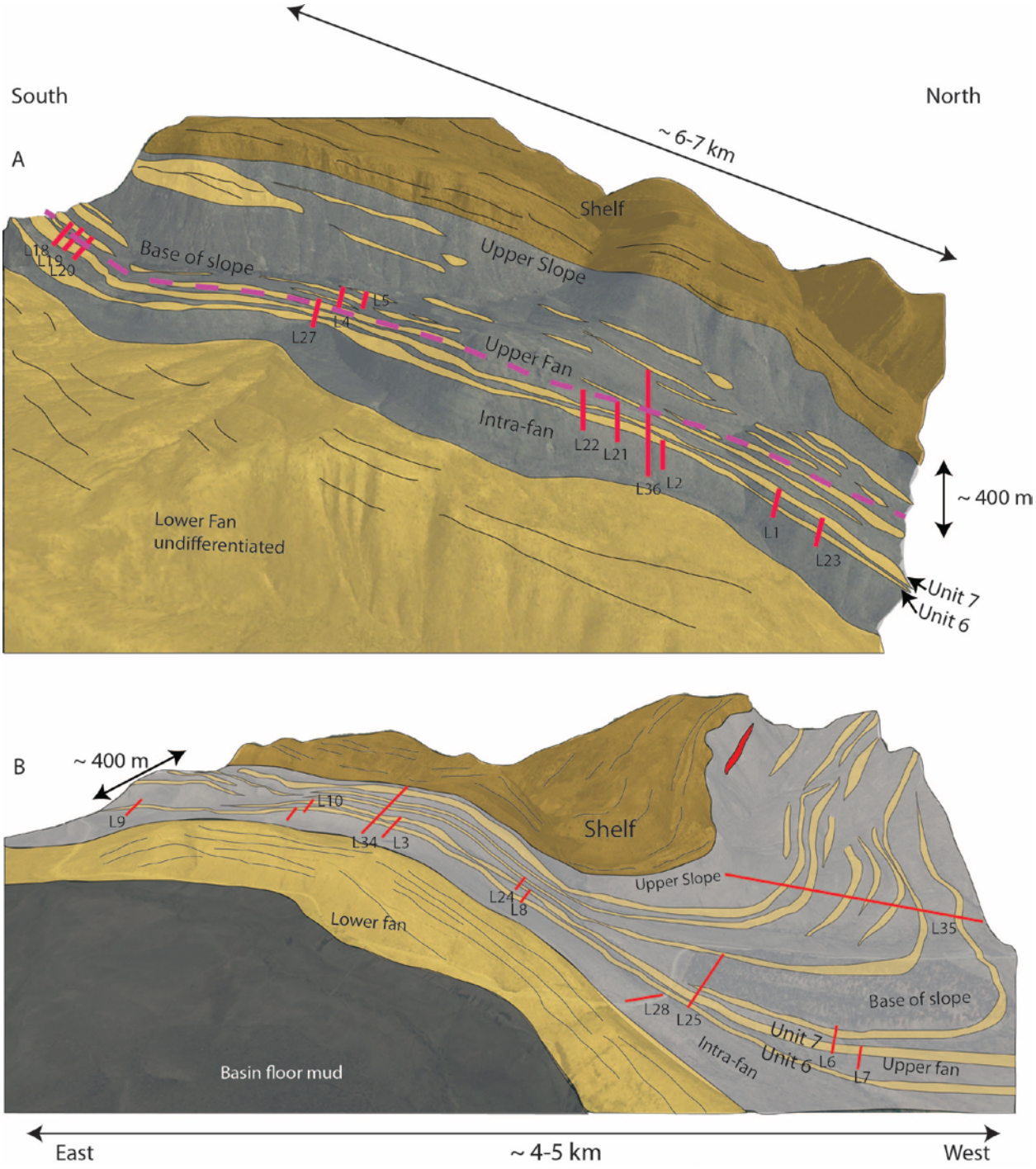

Figure 11 Deep water architecture illustrated in oblique down dip and along strike profiles in La Jardinera area, showing two different basin floor fans (the lower fan undifferentiated) separated by an inter-fan mud dominated interval and the channelized slope and shelf deposits (not studied) and red lines show location of measured sections. In dark red, intrusions are piercing the slope deposits.

4.2.1. Slope channels

In the upper part of the Los Molles slope large channel complexes (Figs. 11, 12 and 13A) have been recognized (aspect ratio 6:1, height: 200m and width: 1200m), with multi-story channel complex fill, dominated by conglomeratic and sandstone beds, amalgamated and stacked, with multiple incisions. From proximal (south) to distal (north) we observe a transition from upper slope channel complexes towards middle slope complexes, and there is a downslope change (decreasing by about x4) in aspect ratio down-slope. The common infill of the confined channels is amalgamated, coarse to very coarse grained sandstones along the channel axis, thin mud drapes at erosional contacts and pebbly conglomerates at the base (Vann, 2013). The net-to-gross ratio for these channels is very high, 85-90 % in the axial part, decreasing lateral to 45-60 % (Vann, 2013).

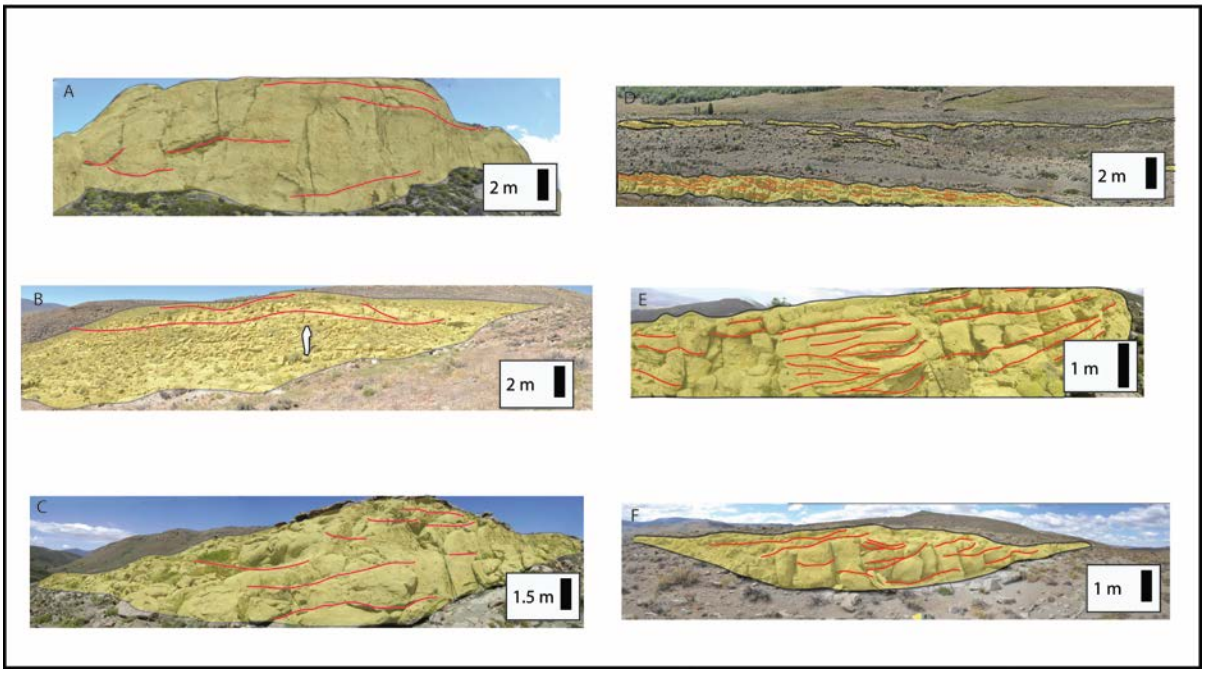

Figure 12 full caption next page

Figure 12 Channel evolution from upper slope to basin floor with changes in width to height ratios from confined to unconfined: A. Upper Slope Channel Complex, W: H: 1200-200m (larger in reality than shown in the photo), B. Middle Slope Channel Complex, W: H: 50-20m, C. Lower Slope Channel, W: H: 20-3 m, D. Scours, W: H: 150-2m, E. Weakly confined channels, W: H: 1000-20 m, F. Channelized lobe, W: H: 3000-20m (the channels do not follow the same timeline)

4.2.2. Transitional zone from slope to basin floor

The toe of slope area represents the transition from a low-angle (2-3 degrees) slope to almost flat (less than 1 degree) basin floor. In terms of depositional architecture, this represents the transitional zone between channels and depositional lobes. The erosional channels have simple to complex margins, contain an axial infill of pebbly conglomerates, and show an upward thinning pattern of sandstone and siltstone beds that contain common internal erosion surfaces (Fig. 13B). At the base of the slope smaller secondary flow pathways carved into the substrate as gullies, draped by mud-clast conglomerates. Increased slumping can be observed in the lower part of the slope (see also Paim et al., 2008), due mainly to the change in gradient (Figs. 8 and 10). The mudstone-dominated intervals are likely to be an indication of periods of avulsion or deposition from the bypassing turbidity currents tails.

From slope to basin floor, on large scale, we observe changes in geometries from confined lower slope channels to semi-confined channels in an oblique down dip profile (Figs. 11 and 14, see also Vann, 2013). At the most proximal part (south) of the outcrops we recognize an area (~ 4 km dip oriented) characterized by discontinuous erosional sandstone bodies, amalgamated and non-amalgamated, with a widespread distribution., The base of these bodies define different types of scour (amalgamated or isolated). The scour dominated area indicates sediment gravity flows bypassing towards the north (basinward). Down-dip from the bypass area

(Fig.14), weakly confined channels, slightly erosional along the axis but depositional in the off-axis areas, are cutting into the muddy substrate or into thin bedded heterolithic mudstones and sandstones. The area with weakly confined channels is not extensive, only ~ 1.5 km in length, transitioning down dip into a zone dominated by amalgamated sandstone units, sand rich, with a clear increase in bed thickness and grain size. The amalgamated zone crops out along a strike profile for approximately 1-2 km, decreasing in thickness laterally from west to east. Further away, 3-4 km northwards, and interpreted as distal basin-floor fan mudstones, following the down dip profile an outcrop belt orientated W-NW-E-SE (Fig. 7) exposes the lateral equivalent deposits. Within this outcrop there are thickening upward packages that may be time equivalent with the zones pertaining to the channel-to-lobe transition zone, described below.

4.2.3. Bypass/ Erosional Area

The characteristics of a bypass area can be deduced where noticeable shale to sandstone ratio change occurs, where thicker inter-sandstone units of mudstone occur, and where more unconfined sandstone units separate from discontinuous confined sandstone units. The by-pass area associated with lobes (units) 6 and 7 of the upper fan (Figs. 14, 15, 16 and 17) was defined by the changes in sandstone beds from confined channel infill into more unconfined scour fill, with widespread and irregular geometries (elongated, ellipsoid, amalgamated), varying in length from tens of meters to hundreds of meters and with beds having under 0.5 meters in thickness. The dip-oriented outcrops are found 4 km south of National Route 46, in the Beymalek Estancia (Figs. 7, 11A and 14). Within this area a low net to gross ratio (20 % per sandstone unit), with a vertical decrease in sandstone content from basin floor to slope and a change in geometry from continuous sheets to discontinuous channels (Figs. 11 and 14) is observed. Muddy matrix debris flows are recognized within the thin bedded mudstones, possibly as a result of slope failures.

In order to define the bypass area, erosional surfaces and bypass indicators were used. The proximal basin floor records erosion and sediment bypassing, thin channelized deposits, (3-4 m thick), small local scours filled with coarse grained sandstone which contain common mud-clasts (Facies A), indicating upstream erosion. Other bypass indicators are the occurrence of coarse lags, 0.2-0.5 cm scour infill, associated with an increase in mud-clast content at contacts and sometimes at the top of the beds.

4.2.4. Weakly confined channels

On a down dip profile from the southern outcrops in Beymalek Estancia, crossing a high relief hill defined by an intrusion piercing through the Jurassic deposits (Miocene Naunauco volcanics) the two continuous units cropping out (lobes 6 and 7) are interpreted as weakly confined channels, because of their marked erosional bases (Figs. 14 and 18). The deposits transition from confined channels on the lowermost slope into a bypass dominated zone of weakly confined channels (Fig. 14). The latter were filled with thick-bedded, 10-12 m, amalgamated sandstones (Facies B, Fig. 15) along the axis and thinner, normally graded (Facies C, Fig. 15) 0.3-0.5 m thick beds, in the off-axis part (Fig. 15). The weakly confined channels have the tendency to be filled from axis (N:G 70 %) to off-axis (N:G 35 %) by amalgamated, thick-bedded (0.5-1 m) structureless sandstones (Fig. 18) which would suggest a rapid infilling of channels by high-density concentrated gravity flows. A decrease in amalgamation can be observed towards the channel margins and an associated increase in normally graded (Facies C) and planar laminated sandstones (Facies D). The channels are interpreted to have been formed in a proximal basin floor setting, based on (1) the absence of associated thick heterolithics bounding them (Facies F), (2) a decrease in confinement for channelized flows (high aspect ratio), and (3) a lack of bypass indicators (incisions). Weakly confined channels are lenticular,

with low relief erosional surfaces and with coarse grained lags commonly found along the base of major erosion surfaces, with mud-clast conglomerates (Fig. 9) accumulating at the base of the beds, on top or throughout the bed. In the weakly confined channels off-axis area, thinner beds that consist of non-amalgamated structureless sandstones (0.5 to 1m) to normal graded and/or planar laminated sandstones are laterally associated with axial deposits. Weakly confined channels represent the continuation of confined channels, with broader aspect ratios, previously described as weakly confined channel complexes (Brami et al., 2000, Brunt et al., 2013).

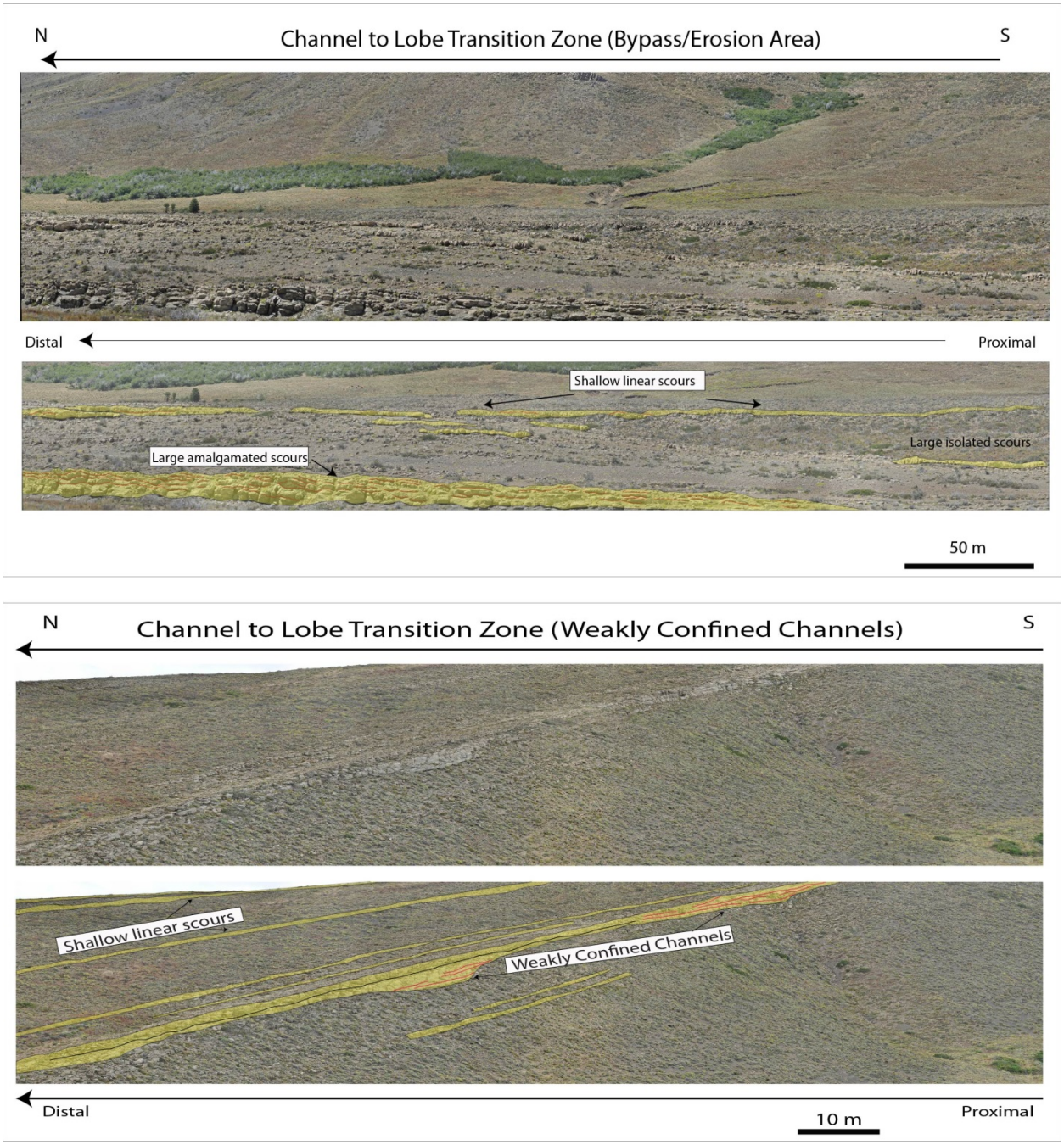

Figure 13 High resolution photo-panorama of the bypass/erosional area in Beymalek estancia and photo-panorama of the weakly confined channels area in Beymalek estancia

4.2.5. Zone of highly amalgamated sandstones

In the units within the upper basin floor fan, 6km downslope from the possible break of slope, we observe a marked increase in thickness of the sandstone units, an increase in amalgamation (3-5m thick), with a slight increase in grain size (medium to coarse sand). Occasional pebble conglomerates (debris flows) (Fig. 9.3) associate with the proximal end of the units. Most of the beds are continuous, amalgamated and thicker where the axis of the weakly confined channels occurs, orientated towards the north-north east. The amalgamated area crops out on a strike profile (Fig. 11 and 14), with a vertical transition from continuous, unamalgamated sandstone beds to more amalgamated, coarser grained, thicker sandstone beds, with the upper levels interfingering with debrites. Above the thick amalgamated sandstone zone we transition into thick mudstone intervals with rare scours (50-70cm thick) and soft deformed beds (Facies E, slumps) related with the next mapped unit. Vertically this corresponds to a change in net to gross ratios (70 % to 20 %), confined channels, and thick muddy intervals (~ 10-20m) separating the units.

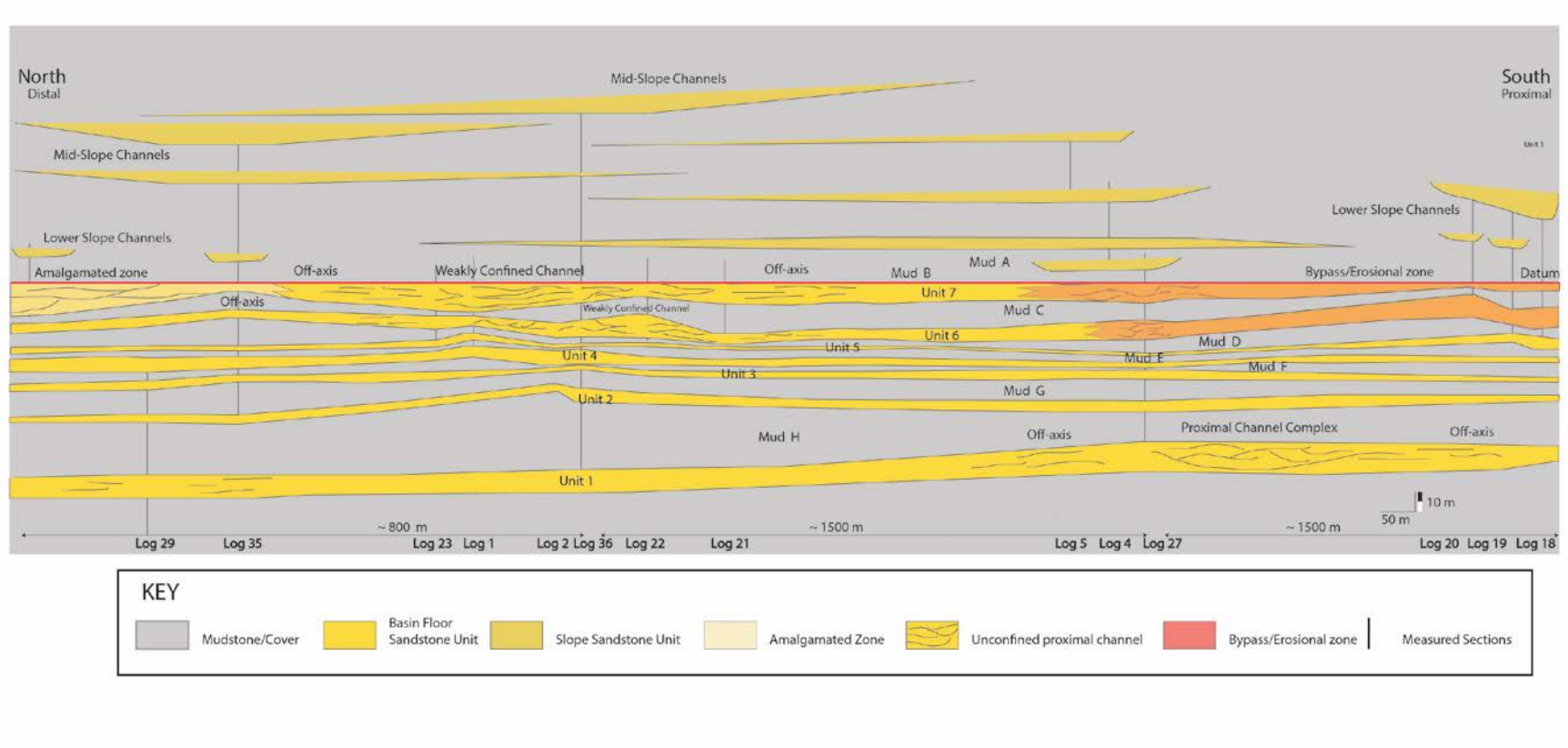

Figure 14 Down-dip correlation panel between measured sections showing correlated mudstone intervals and the different architectural elements (bypass zone, weakly confined channels and amalgamated zone). The transition area between the bypass zone and the weakly confined channels is mostly covered, it is only implied from regional data (satellite image, paleocurrents and high resolution photopanoramas)

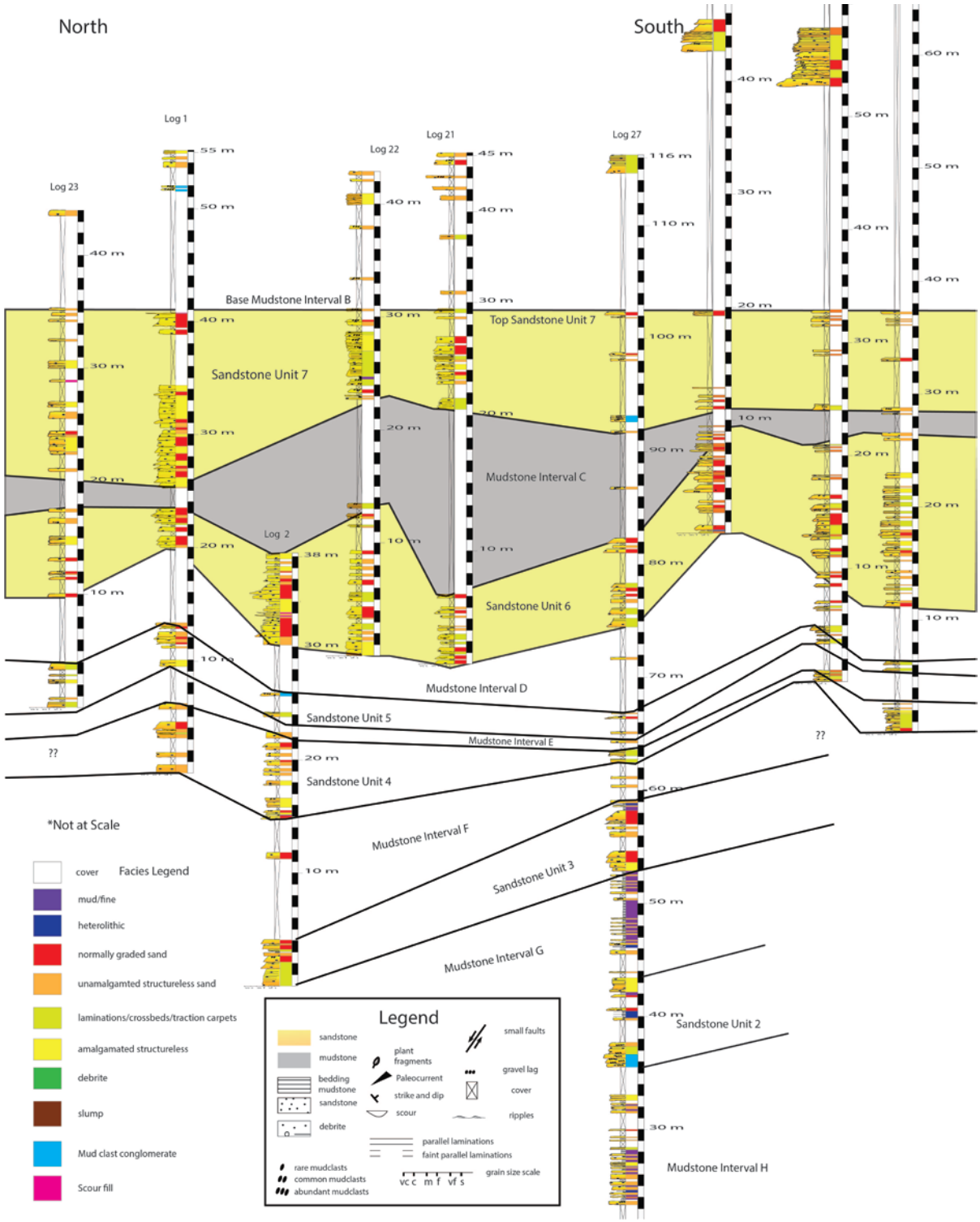

Figure 15 Down-dip correlation between measured sections showing correlated mudstone intervals focusing on the two studied units (6 and 7)

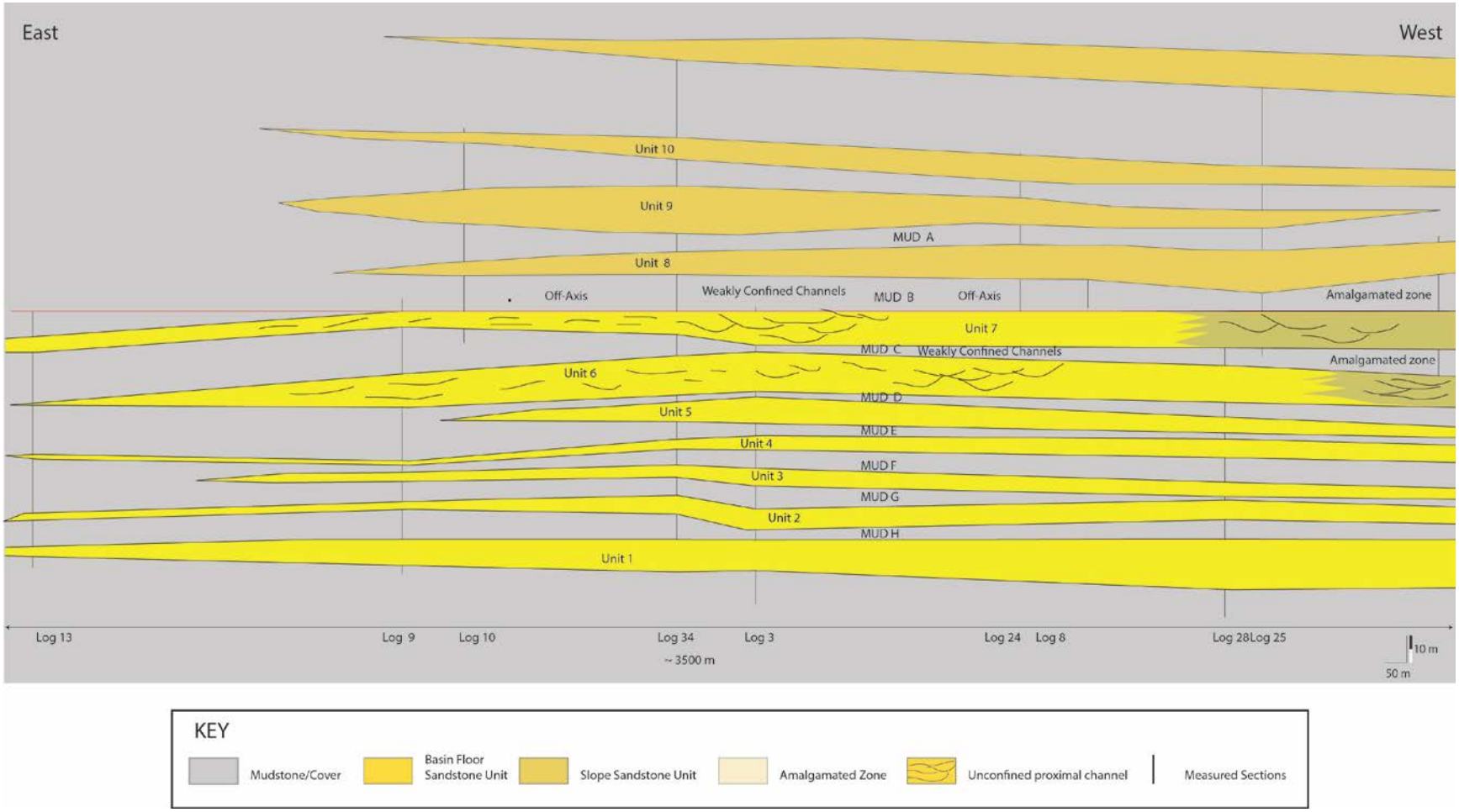

Figure 16 Along-strike correlation panel using measured sections and showing the different architectural elements found (weakly confined channels)

4.2.6. Channelized Lobes

The proximal basin-floor channelized lobe complex is defined based on recognizing related areas of erosion and sandstone amalgamation using high resolution photo-panoramas for geometries (Fig. 13, 21), and measured sections for detailed facies observations. Down dip in the proximal fan system, channels with very low relief erode the upper most part of a depositional lobe. Towards the top of the lobes we observe more amalgamated beds (Facies B), with trough cross-laminated sandstones (Facies D) that can be interpreted as scour and fill facies. Sharp based normal graded beds can be seen often, inter-channel areas are thinner, and beds are less amalgamated.

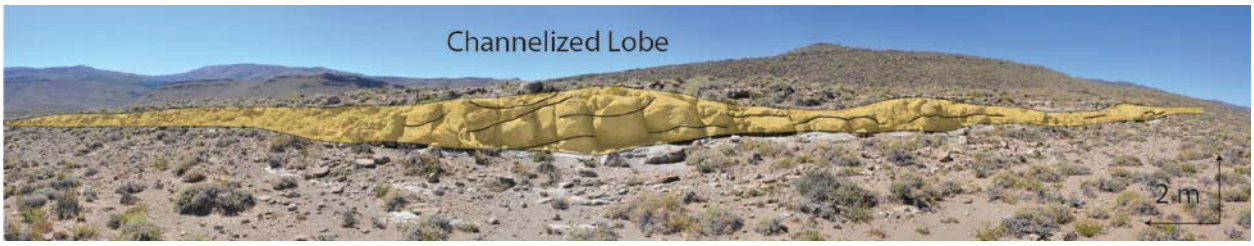

Figure 17 Photo-panorama showing lateral thickness changes in a channelized lobe, 4 km North from the down-dip correlation panel

4.2.6.1. Lobe complex

Lobes are laterally constrained within the sand-rich area on the top of a fan transitioning laterally/distally into the lobe fringe (Mulder and Etienne, 2010). They are the continuation of weakly confined channels, with little to no erosion occurring within the lobe. Laterally thick-bedded non-amalgamated sandstones (Facies B) can be traced and there is little or no presence of channel lags or mud-clasts. These deposits show an increase in aspect ratio (height:width), compared to the more confined pattern at the base of slope.

The basal mudstone (Facies F) part of each package marks a period of lobe shutdown in the earlier phase of fan building, recorded by thinner, fining upwards successions. Its presence and thickness is dependent upon the degree of avulsion experienced by the subsequent lobe.

An increase in coarse grained lag deposits can be observed in the most proximal area (bypass/ erosion area) within the channel-to-lobe transition zone (Fig. 13) and it can be associated with the change in gradient at the base of slope and/or high energy erosional flows, with common lags and mud-clasts attributed to major and minor erosional surfaces. Evidence for transitioning from confined to unconfined is observed on a vertical profile with an increase in mudstone content from basin floor to slope.

4.2.6.2. Lobe Fringe

The fringe area is defined by the increase and abundance of fine grained interbedded sandstones and mudstones in relationship with an increase in shale to sand ratio distally on the lobe. The fringe is recorded in the basal part of axial or non-axial thickening/thinning upwards succession of lobes. From field mapping, the distal muddy part of the study fan has a thickness more than 100 m. However, the muddy intervals on the slope present similar facies. In order to distinguish the inter-bedded sandstones and mudstone on the basin floor from those on the slope, observations on sand to shale ratio increases and decreases and lateral relationships of sandstone units (lobes or channels) were essential. The thin bedded facies of intervals (Facies F) of fringe deposits are usually rippled and planar laminated, and they are rich in ammonites and bivalves and with occasional debrites interfingering with the deposits. As part of the lobe commonly thickening upward packages (10-15 m thick) the fringe represents approx. 6-8 meters of the package, varying across the fan, with thinner intervals associated with main paleoflow axis.

4.3. FACIES VARIABILITY OF LOBE 6 AND LOBE 7 OF THE UPPER FAN

4.3.1. Geometry characteristics

A transition from scouring to erosional channels was discerned, represented by weakly confined channels (W: H 500 m: 10 m) and dominated by amalgamated sandstones beds, with common basal lags and mud-clasts clustered at erosional contacts. Into the more depositional part of the fan, we recognize an increase in normally graded beds (from 30 % to 50 %).

Unit 6 corresponds to the lower, older unit, already defined as more proximal than unit 7. Based on the observations made on the two lobes mapped across the area, the transition zone between channels and lobes is characterized by three sub-zones (Figs. 14, 16 and 24). Main factors that drive these differences are N: G ratio, increase of bed thickness and grain size and certain facies clustering (amalgamated structureless sandstone and mud-clast conglomerates).

Overall the vertical profile through the entire upper fan shows a thickening upward trend. Notice that we do not intersect each unit in its axial position. We distinguish deposits of the axial position of a lobe from the deposits representing off-axis deposits or fringe deposits based on thickening upwards and thinning upwards trends and relationships (Fig. 18).

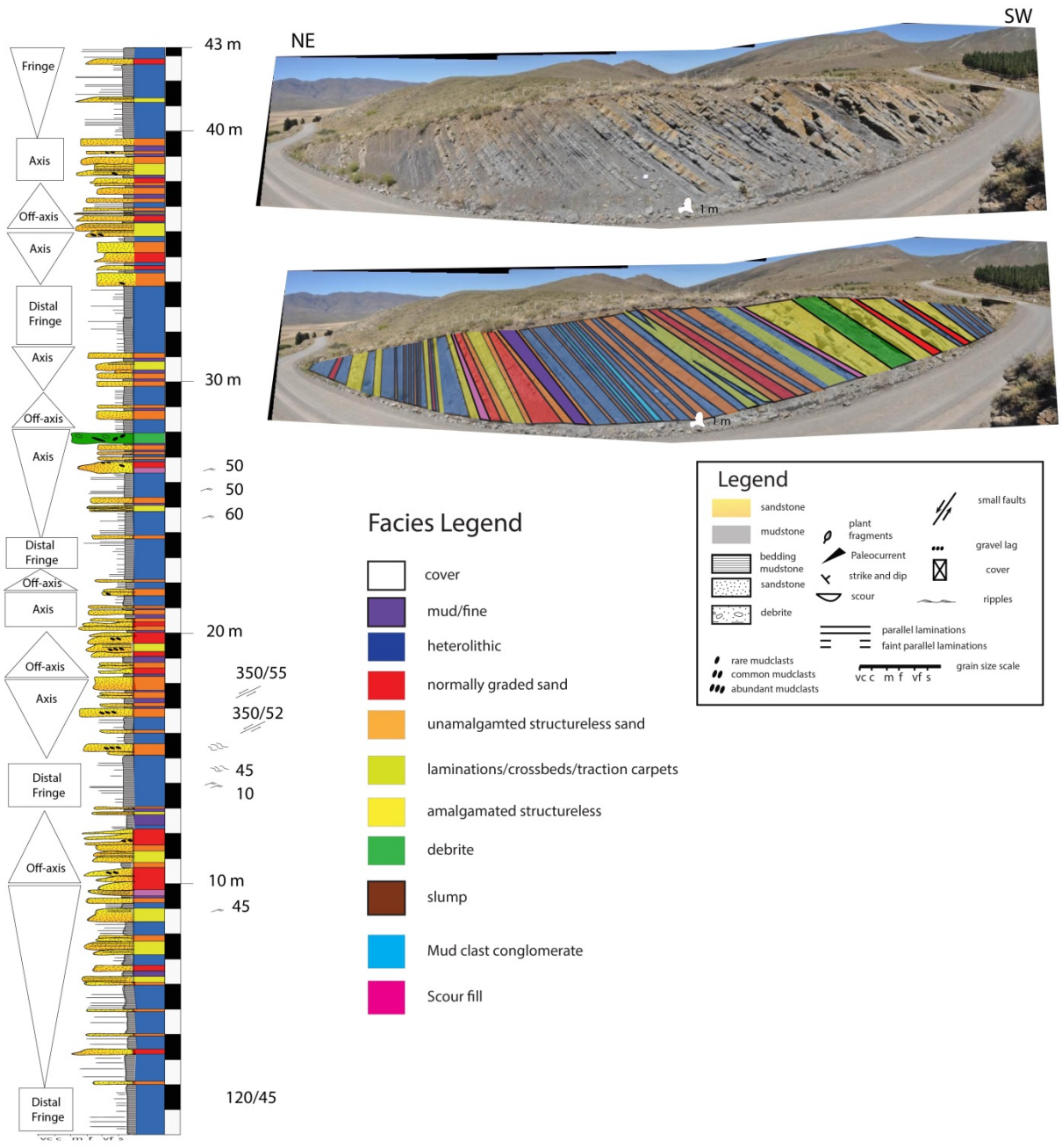

Figure 18 Photo-panorama with L28 measured section showing vertical outcrop profile of the upper fan, illustrating the vertical separation for lobe axis and off -axis from fringe and distal fringe.

4.3.2. Bed thickness and grain size

Within the unit 7 (Figs. 19, and 21) there is an increase in average bed thickness (10cm to50 cm) and grain size (fine to medium) was observed. Laterally, eastward, a decrease in bed thickness (1 m to 0.5 m) and in grain size (medium to fine) for the units (Figs. 21 and 22) occurs. Unit 6 (Figs. 20, and 22) corresponds to the lower, older unit defined as more proximal than unit 7. Similar patterns were recognized, with a clear increase in bed thickness (0.5 to 1 m) and very little variability in grain size (medium grained).

On the vertical profile, deposits transition from the inter-fan mud dominated interval, into a sandstone dominated interval, with thin-bedded intervals thickening into more continuous beds, with depositional and non-amalgamated units, localized debrites interfingering with the sandstone units (lobes). Towards the top of the profile, thicker and more amalgamated beds are dominant with less fringe deposits occurring.

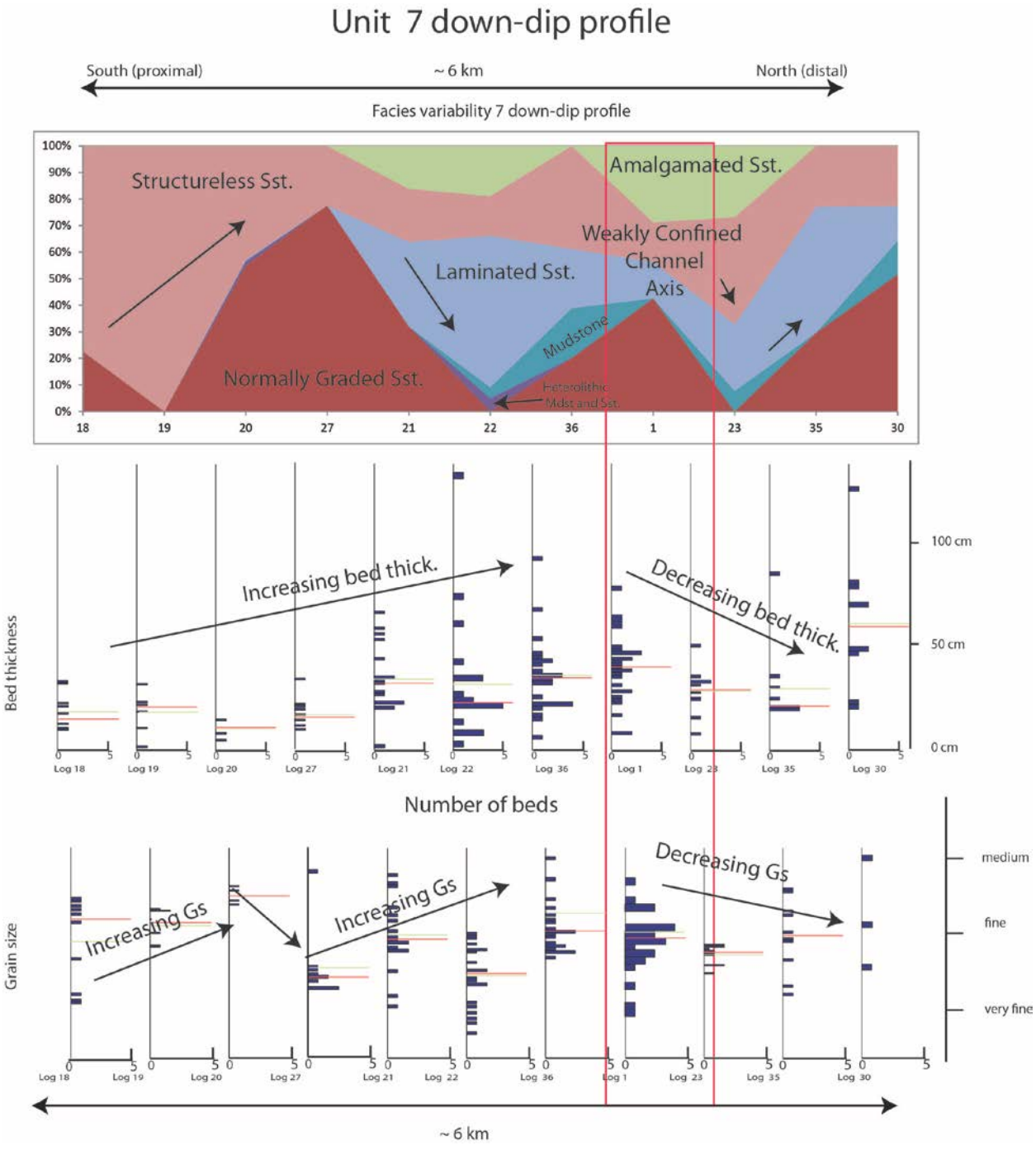

Figure 19 Facies, bed thickness and grain size changes om am oblique down-dip profile (Unit 7), (average 50cm thickness and upper fine to medium grain size changes), transitioning from axis to off-axis (see Figs. 14 and 11 for location)

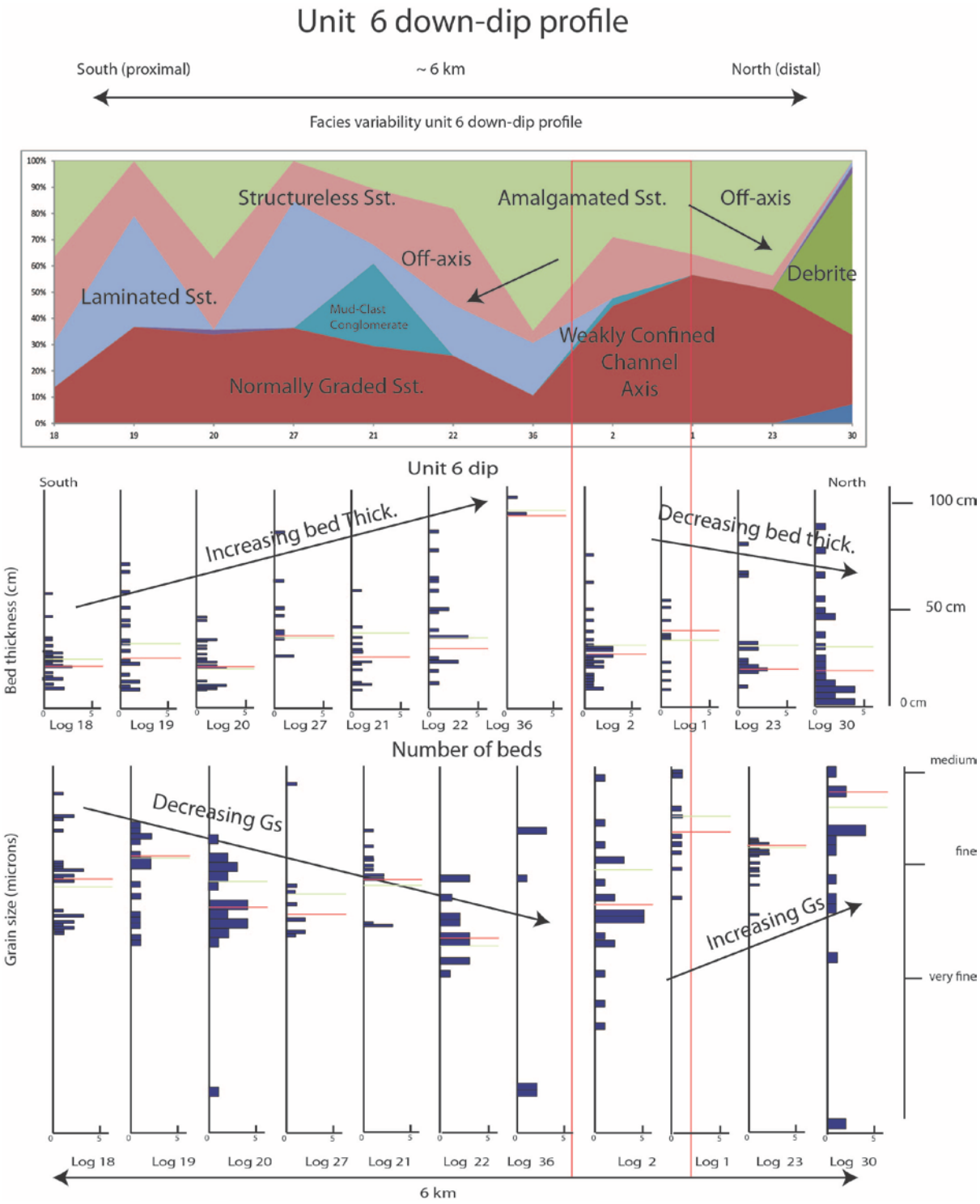

Figure 20 Facies, bed thickness and grain size changes along a strike profile (Unit 6) (bed thickness and grain size decrease from west to east), (see Figs. 14 and 11 for location)

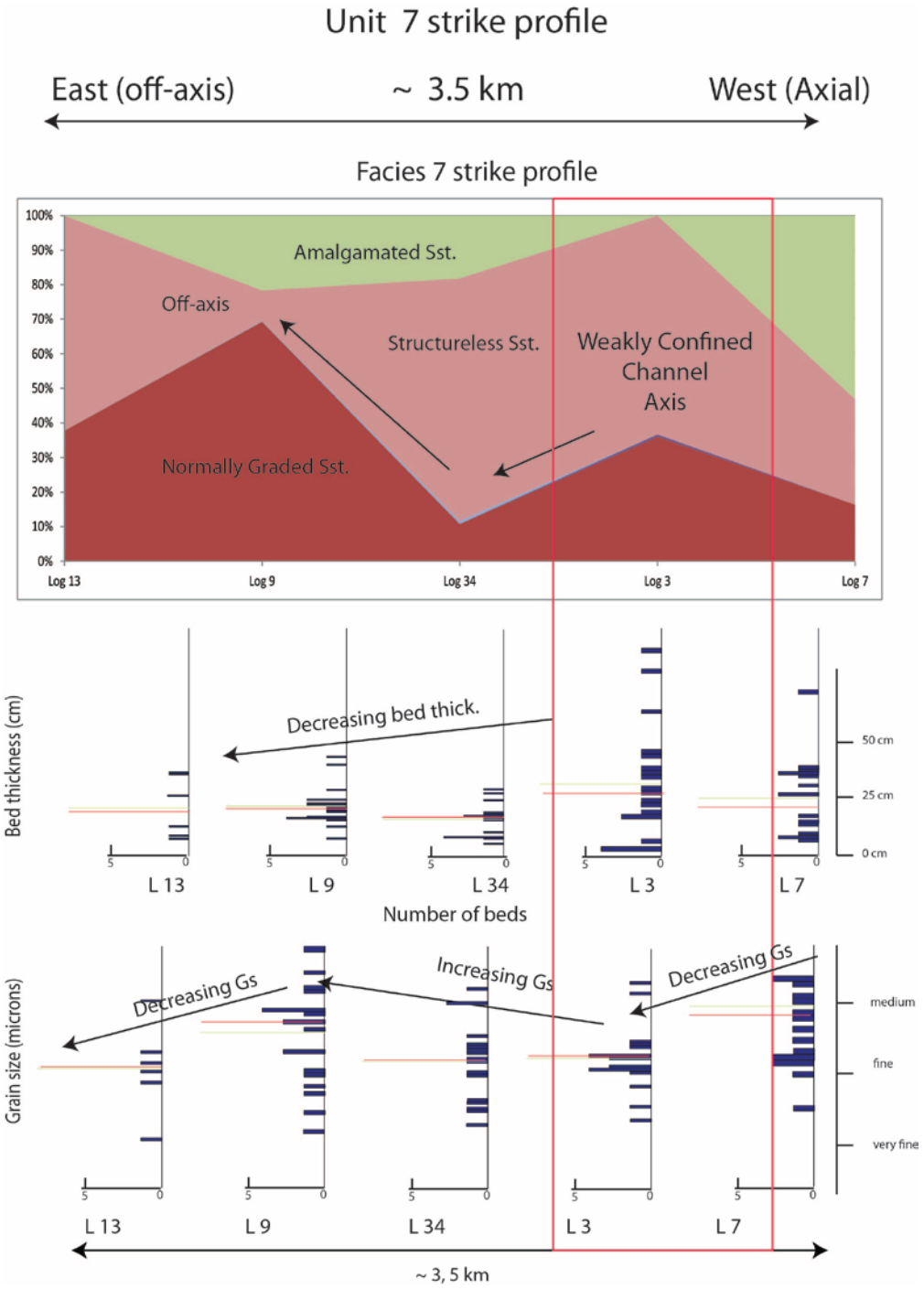

Figure 21 Facies, bed thickness and grain size changes along a strike profile (Unit 6) (bed thickness and grain size decrease from west to east), (see Figs. 16 and 11 for location)

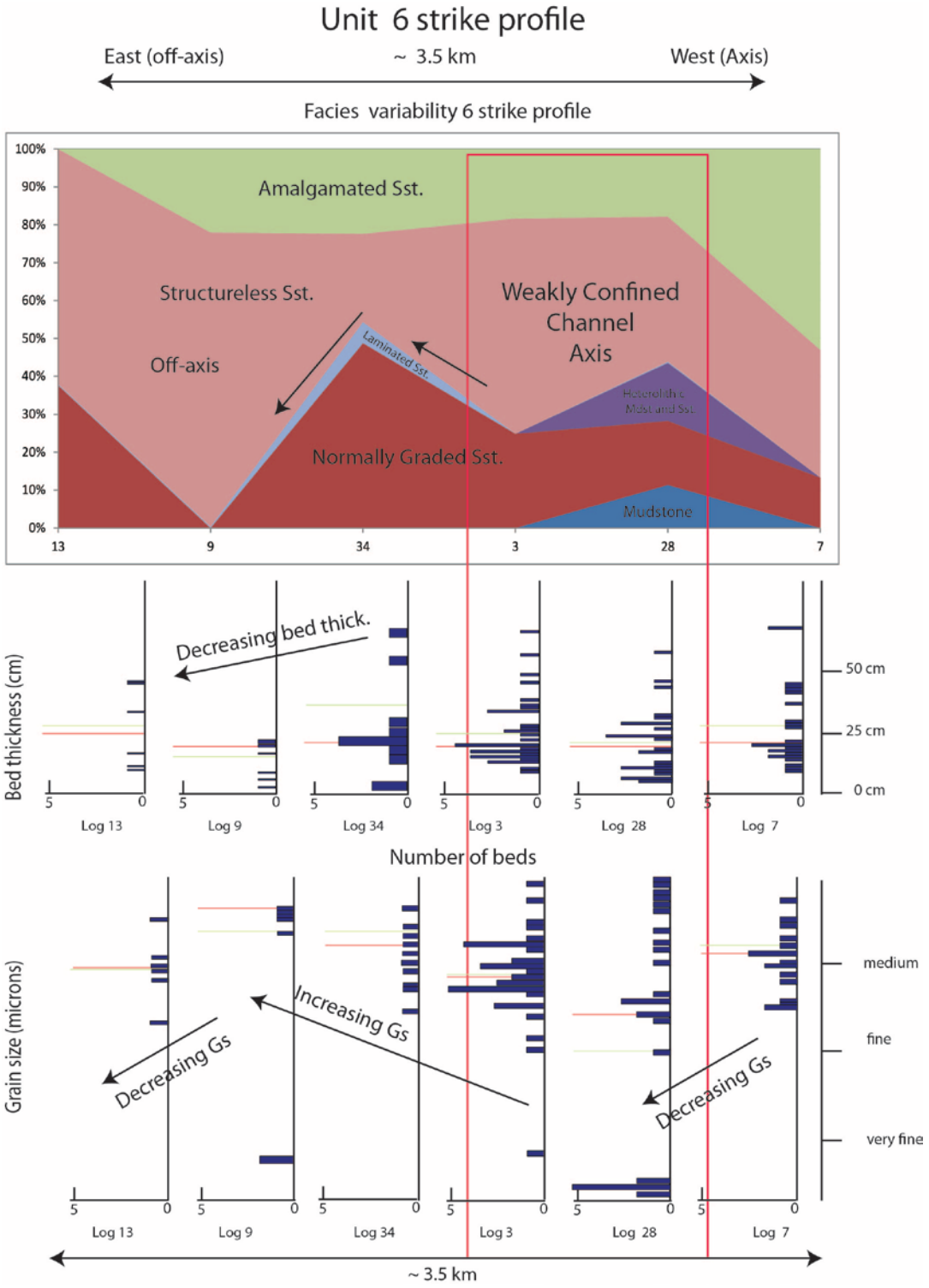

Figure 22 Facies, bed thickness and grain size changes along a strike profile (Unit 6) (bed thickness and grain size decrease from west to east), (see Figs. 16 and 11 for location)

4.3.3. Facies distributions

Within the unit 7 from the most proximal part, dominated by amalgamated and non-amalgamated structureless sandstone (80% in the bypass area to 20 % in the proximal channels) forming isolated and amalgamated scours. Using Matlab facies distributions along dip and strike were plotted (Figs. 19 to 22) and through that we could observe the dominance of amalgamated structureless sandstones in the axial part of channels in the proximal channels area and in the amalgamated zone. It is usually associated with mud-clasts and basal lags. When observing facies changes, an increase in normally graded and planar laminated sandstones in contrast with a decrease in structureless sandstone, towards the East, away from the main axis (N-NE) is noticed. Scours are observed in the proximity of the break of slope, widespread and low relief erosional features, common amalgamated down-dip.

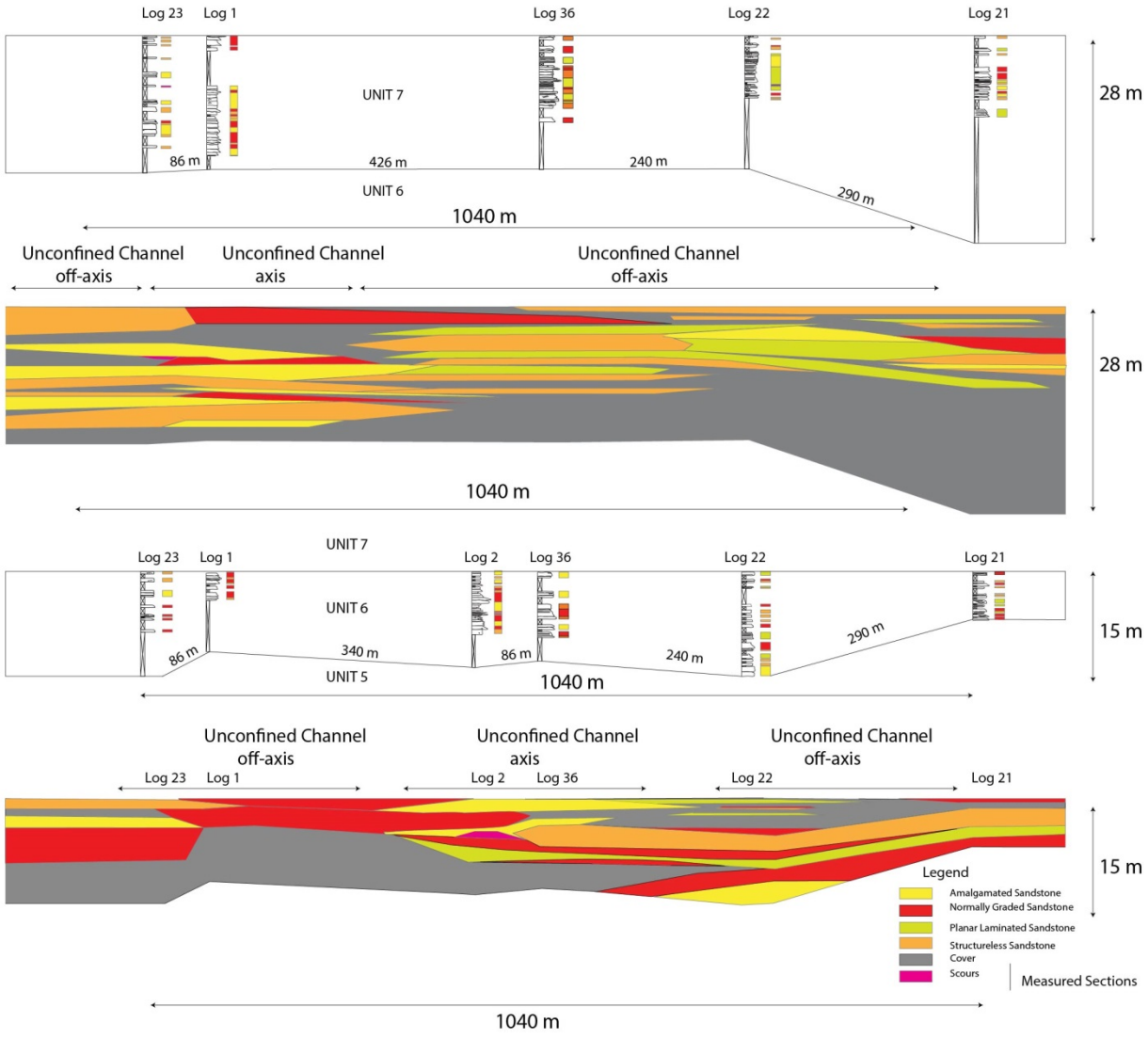

Figure 23 Lateral and vertical facies changes within unit 6 and 7, focusing on the weakly confined channels, with small thickness and facies shifts from right to left (unit 6) and from left to right (unit 7)

There are important differences between the two units (Fig. 23), such as the presence of debrites in unit 6, in the down dip, off-axis area, interfingering with the lobe fringe. The increased amalgamation of sandstones was noticed shifting from left to right (unit 7) and from

right to left (unit 6). The overall geometry of the unit was used as indicators for transitioning from the bypass/erosional area to the weakly confined channels. Laterally, a clear decrease in average bed thickness (1m to 30cm) and average grain size (medium to upper fine).

Using the measured sections, isopach maps were created (Fig. 24) for the two units (6 and 7). The data was associated with grain size and bed thickness distributions and overall interpreted based on the field observations on changing geometries.

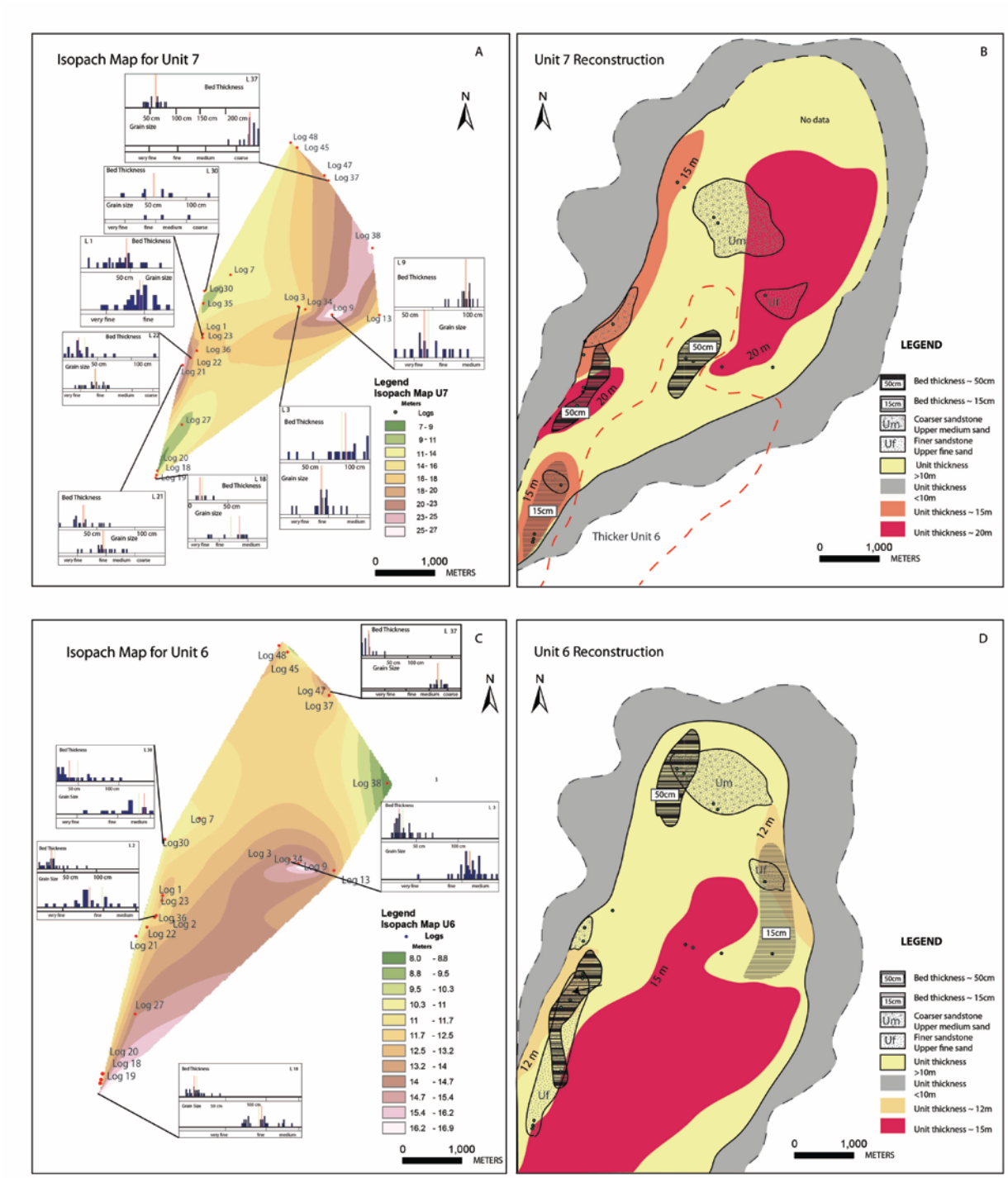

Figure 24 full caption next page

Figure 24 A and C. Isopach map for unit 7 and unit 6 with bed thickness and grain size averages plotted at different locations showing the regional variability within unit 7. B and D. Reconstructed map for unit 7 and unit 6 based on bed thickness and grain size distribution associated with field observations (the different patterns show the variability). Observe the thickness variation between the two units suggesting progradation from unit 6 to unit 7

5. DISCUSSION

Comparison between architecture changes from slope to toe of slope and between the toe of slope to basin floor is made below. Also, the Los Molles Fm. deposits are compared with other deep water deposits in similar depositional settings.

5.1. ARCHITECTURE CHANGES FROM SHELF EDGE TO SLOPE TO TOE-OF-SLOPE TO BASIN FLOOR

The shelf and slope deposits were briefly described and interpreted in previous studies (Paim et al., 2008; Vann, 2013), illustrating sharp changes from conglomerate dominated shelf margin into confined upper slope channel complexes into sandstone dominated slope channel infill, with mud-drapes and coarse grained bases. A change in gradient occurs at the base of slope, although the transition is less defined (Fig. 8 and Fig. 10).

Shelf-margin clinoforms similar in height (200-300m) to those described in the Spitsbergen Tertiary Basin (Eocene) (Johannessen &Steel, 2005; Uroza & Steel, 2008), are observed in the La Jardinera outcrop belt. The La Jardinera outcrops show evidence that the system has a wide grainsize range, with conglomerates on the upper slope and shelf and usually coarse grained sandstones in the lower basin floor fans (Paim et al., 2008, Vann 2013). Bouma et al., (2000) defined coarse grained systems as non-efficient for basin transport (e.g. Gulf of Corinth, Poulos et al, 1996), with a progradational style and a net-to-gross ratio that decreases lateral from sediment pathways. Particularly, in coarse grained systems lobes are mounded, composed of medium to coarse grained amalgamated sandstone, and scours and low relief channels may still affect the top of the lobes in the proximal part (Galloway, 1998). In the study area, we have observed scouring still occurring well onto the basin floor fan, affecting the upper parts of the lobes (Fig. 17).

5.2. CHANNEL-TO-LOBE TRANSITION OF LOS MOLLES COMPARED WITH PREVIOUS MODELS

The channel-to-lobe transition zone is characterized and defined by Wynn et al., (2002) in four different scour dominated areas following observations in the modern environments (e.g. Agadir Fan, Lisbon Fan, Fig.1). Similar, the channel-to-lobe transition zone in the La Jardinera outcrops is characterized by a series of erosional scours of various sizes and weakly confined channels that are feeding lobes which can be channelized or non-channelized. In terms of size, the channel-to-lobe transition zone is roughly proportional to the size of the turbidite system (Wynn et al., 2002). In the study area we recognize that the transition zone is roughly 4-5 km in length within a larger fan which is probably about ~ 30 km in length (the outcrop extent is less than that).

Based on studies in the Karoo basin, the depositional transitions of units with overall tabular sheet geometry with internal scours and very minor channelization are present in areas on the fan where the flow changes from confined to unconfined nature (Johnson et al., 2001, Brunt et al., 2013). In the La Jardinera outcrops we can observe where the deposits change from a bypass scour intensive area into minor channelizations and internal scours into tabular sheet geometry within continuous sandstone units, delimiting these changes into the bypass area/ weakly confined channels and channelized lobes.

In the mud-prone submarine fans, Ito (2008) suggested that a deposit formed at the channel-to-lobe transitional zone has more potential to undergo flow transformation and thus could be used as a characteristic of channel-to-lobe transition zone in outcrops. Ito (2008) interpreted that due to an associated hydraulic jump or a thinning of the precursor turbidity currents, these would have led to the incorporation of finer material that would have suppressed the flow turbulence transforming it into a laminar flow. Most likely, the flow expansion that

happens at the channel-to-lobe transition is the one that drives flow transformation and facies variability (Kane and Ponten, 2012). Flow expansion between confined and unconfined flow was observed in modern environments, shown by repeated erosion, defined by scours, amalgamated and isolated immediately downslope from canyon/channel mouths (Wynn et al., 2002). The flow confinement changes downslope and also leads to different geometries (from erosional channels to mounded lobes). In this study, the focus was more on facies variability from channel-to-lobe and with a diminished focus on flow transformation, mostly because of rock exposure and bed continuity. The only observations for flow expansion were made based on bed thickness changes from proximal to distal, increasing towards the center of the lobe. In the central parts of the lobes dominant thick sandstones with sharp bases to increasing amalgamation and scouring were observed. These thickening upwards packages that were bounded by "rich" mudstone intervals at the top would be the axial parts of the lobes, based on comparisons with deposits from the Karoo Basin (Prelat et al., 2013) and from Ross Formation (Macdonald et al., 2011).

Other important factors in understanding the transition zone are bed thickness and continuity, grain size distribution and facies variability. The grain size distribution is considered to be controlled mainly by depositional processes, with slides, slumps and debris flows having sufficient strength to carry any particle for long distances while the turbidity current cannot do that, due to their deficiency of strength (Shanmugan, 2006). In East Corsica late Pleistocene deepwater fans the maximum sediment accumulation occurs between 0 and 5 km, with coarse grained lobes and with thicknesses ranging between 9 to 20 m (Deptuck et al., 2008). Similar with the dimensions described in East Corsica, in La Jardinera area, the lobes are coarse grained and largely amalgamated, with thicknesses ranging between 10 to 20 m. The area covered by the lobes cannot be determined due to outcrop limitations. In the La Jolla fan system, a similar

scenario with the one in La Jardinera area occurs, where sediments become coarser down fan, mainly due to the strength of the high-density currents, indicating that the fan is dependent on sediment supply rather than on sorting by the transporting current (Piper, 1970). Bed thicknesses are influenced by several factors such as flow trigger mechanisms, from oversteepening slope, seismic destabilization or direct fluvial discharge, and flow rheologies, which depends on grain size distribution and flow hydrodynamics (Sinclair et al., 2003) . In La Jardinera area, Paim et al. (2008) defines the toe of slope based upon the "slope rise" slump deposits exclusive occurrence that could also indicate the beginning of the transition zone. We consider that the occurrence of slump deposits is not the only indicator for the slope break but also the vertical change in shale to sand ratios and lateral changes in geometries from confined and isolated channels to discontinuous scours and weakly confined channels to sheeted continuous sandstone bodies (Fig. 8).

Based on previous studies, the expectation was to see coarse grained channel infill with normal grading, debris flows and slumps at the toe of slope with a basin transition into amalgamated sand sheets and sheeted fine grained sand bodies with inter-bedded muds towards the fringe of the existing lobes (Fig. 25). These assumptions are directly related with the flow rheology and existing basin floor topography. The change from slope to basin floor might be related with the change in gradient and net-to-gross distribution of the sand in the system, although local areas show bypass at the proximal part where mud dominates and less sand is accumulated on the basin floor (Fig. 26).

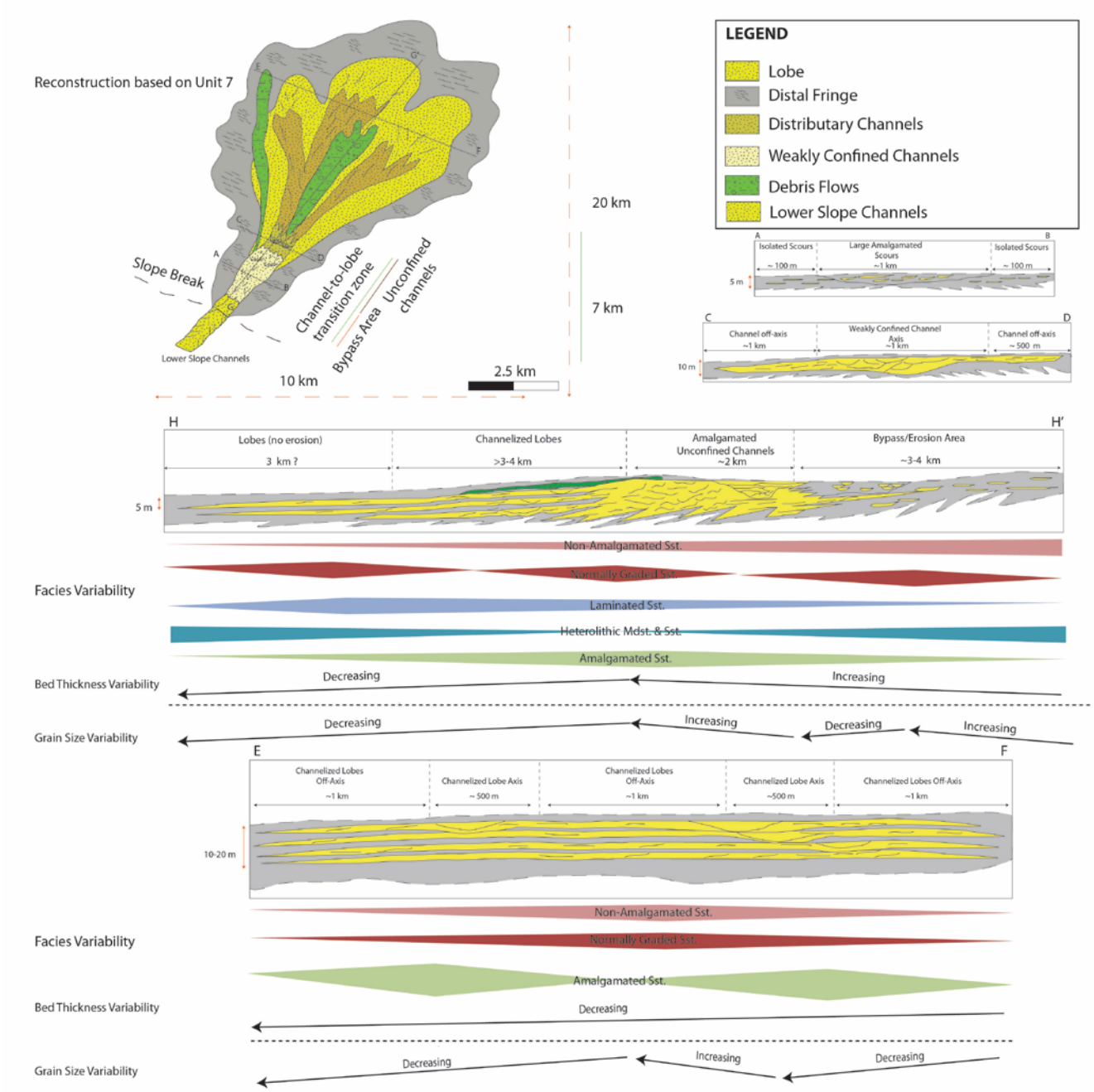

Figure 25 La Jardinera deep water model constructed based on field observations within unit 7, showing a down-dip cross-section with focus on the transition zone, and three intersected sections along strike showing the different changes in width and geometry (from confined to unconfined)

The lobe progradation usually occurs by “lobe avoidance” (Mulder and Etienne, 2010). When lobe elements show a coarsening and thickening upwards sequence, it could indicate lobe progradation (Mutti, 1977). Lobes consist of lobe beds each corresponding to individual depositional beds (0.5-1m thick). Lobe progradation can be argued based on thickness changes for the two units, both showing “lobe avoidance” and infilling the space unfilled by previous lobes.

From current models and field observations a model was created (Fig. 25), emphasizing details recognized in the field, such as: degree of confinement, debris flow presence, coarseness of the deposits and lateral variability of bed thickness and grain size.

The regional model created in order to better illustrate the fan evolution within the system (Fig. 26) shows shallow channels distributing coarse grained sediments throughout the fan, slope channels are discontinuous along any dip section with a decreasing aspect ratio. The outcrops do not show the maximum length for the fan, but following the methodology described by Sømme et al., (2009) and knowing from paleogeographic reconstructions (Ramos, 2008) that the North Patagonian Massif (main sediment source) was roughly 130 km South from the studied area, suggests that the length of the longest river would be at least 130 km. Comparing this assumption with the global data set from Sømme et al., (2009) a prediction on the fan length (~ 30 km) and for the slope length (at least 6-7 km) can be made.

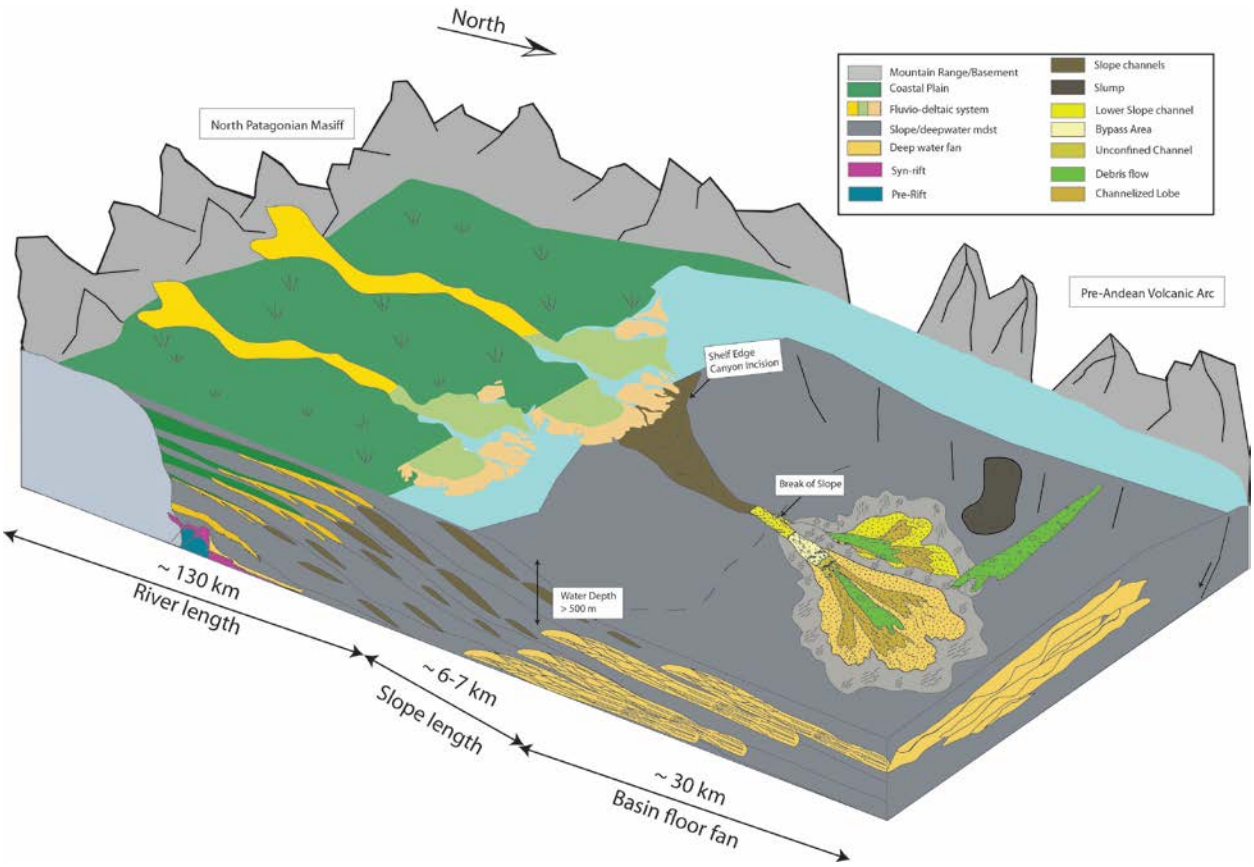

Figure 26 Tridimensional deep water model illustrating the source to sink relationship in La Jardinera area (Challaco-Las Lajas-Los Molles), with focus on basin floor, slope discontinuous channels feeding coarse grained basin floor fans, with long lived channels cutting into the basin floor fan.

6. CONCLUSIONS

The context of the study is a Jurassic shelf-slope-basin floor system (Las Lajas-Los Molles fms.) in southern Neuquen Basin. Focus here was on the lower slope to basin floor transition. Two units were described and mapped in the field along a 20 km long outcrop belt representing the transition from the toe-of-slope channel-to-lobe transition zone out to the depositional lobes of the basin-floor fan. Changes in bed facies, in lobe thickness (from proximal, 8-10 m, to distal, 15-20 m) and changes in grain size (from fine to medium) within the upper fan are documented. The coarsest material was associated with the axial zone of channelized deposits. The downslope facies changes relate to the changes from channel-related erosion to turbidite lobe deposition. Along the lobe-feeding weakly confined channels axes there is increased scour-surface frequency, increased amalgamated turbidite sandstones coarse grained lags and increaseed in mud-clast abundance Along the off-axis areas, normal graded beds and planar laminated sandstones dominate. Debris flows occur within weakly confined channels, within the lobe-fringe deposits or as a capping to lobes. Slumping is common along the break of slope within the thinner bedded intervals and sometimes associated with the weakly confined channels. Distally, the lobes are either channelized or non-channelized, being the terminal reaches of the distributary network of shallow channels on the fan.

The Los Molles Fm. has a thickness of approximately 1000 m. The shelf-margin slope height is calculated to have been ca.400 m (undecompacted), the slope width was about 5-7 km and the basin floor fan cumulative thickness was about 600 m. From upper slope to lower slope the width to height ratio of deepwater channels increased significantly and there was an increase in sand to shale ratio from slope to basin floor from 24% to 74%. The transition zone from

channels to lobes at the base of slope shows a change from weakly confined channels that have a high aspect ratio (height 10-15 m and width 500-700 m) into turbidite sheetsands. Basin-floor lobes thicken upwards in packages varying in thickness from 10 to 15 m and change laterally and down dip from channelized lobes (>600 m in width and 10-12 m in height) to non-channelized lobes.

This study offers new outcrop evidence that the presence of different zones within the channel-to-lobe transition zone can be reasonably well defined in terms of grain size, bed thickness, bed amalgamation and scour-surface frequency changes vertically and laterally.

Appendix

See supplemental CD.

Bibliography

Abreu, V., Sullivan, M., Pirmez, C., & Mohrig, D. (2003). Lateral accretion packages (LAPs): an important reservoir element in deep water sinuous channels. *Marine and Petroleum Geology, 20*(6-8), 631-648. doi: 10.1016/j.marpetgeo.2003.08.003

Bouma, A. H. (1968). Distribution of minor structures in Gulf of Mexico sediments. *Gulf Coast Association of Geological Societies Transactions, 18*, 26-33.

Brami, T. R. (2000). Late Pleistocene deep-water stratigraphy and depositional processes, offshore Trinidad and Tobago. *GSTT SPE Conference and Exhibition*.

Burgess, P. M., Flint, S., & Johnson, S. (2000). Sequence stratigraphic interpretation of turbiditic strata: An example from Jurassic strata of the Neuquen basin, Argentina. *Geological Society of America Bulletin, 112*(11), 1650-1666. doi: Doi 10.1130/0016-7606(2000)112<1650:Ssiots>2.0.Co;2

Burgreen, B., & Graham, S. (2014). Evolution of a deep-water lobe system in the Neogene trench-slope setting of the East Coast Basin, New Zealand: Lobe stratigraphy and architecture in a weakly confined basin configuration. *Marine and Petroleum Geology, 54*, 1-22. doi: 10.1016/j.marpetgeo.2014.02.011

Butler, R. W. H., & Tavarnelli, E. (2006). The structure and kinematics of substrate entrainment into high-concentration sandy turbidites: a field example from the Gorgoglione 'flysch' of southern Italy. *Sedimentology, 53*(3), 655-670. doi: 10.1111/j.1365-3091.2006.00789.x

Cartigny, M. J. B., Eggenhuisen, J. T., Hansen, E. W. M., & Postma, G. (2013). Concentration-Dependent Flow Stratification In Experimental High-Density Turbidity Currents and Their Relevance To Turbidite Facies Models. *Journal of Sedimentary Research, 83*(12), 1046-1064. doi: 10.2110/jsr.2013.71

Clark, J. D., & Pickering, K. T. (1996). Architectural Elements and Growth Patterns of Submarine Channels: Application to Hydrocarbon Exploration16. *AAPG Bulletin, 80*(2), 194-221.

Clayton, C. J. (1994). Contrasting sediment gravity flow processes in the late Llandovery, Rhuddnant Grits turbidite system, Welsh Basin. *Geological Journal, 29*, 167-181.

Deptuck, M. E., Piper, D. J. W., Savoye, B., & Gervais, A. (2008). Dimensions and architecture of late Pleistocene submarine lobes off the northern margin of East Corsica. *Sedimentology, 55*(4), 869-898. doi: 10.1111/j.1365-3091.2007.00926.x

Franzese, J. R., & Spalletti, L. A. (2001). Late Triassic–early Jurassic continental extension in southwestern Gondwana: tectonic segmentation and pre-break-up rifting. *Journal of South American Earth Sciences, 14*(3), 257-270.

Franzese, J. R., Spalletti, L. A., Gomez-Perez, I., & Macdonald, D. (2003). Tectonic and paleoenvironmental evolution of Mesozoic sedimentary basins along the Andean foothills of Argentina (32-54 S). *Journal of South American Earth Sciences*(16), 81-90.

Franzese, J. R., Veiga, G. D., Schwarz, E., & Gomez-Perez, I. (2006). Tectonostratigraphic evolution of a Mesozoic graben border system: The Chachill depocentre, southern Neuquen Basin, Argentina *Journal of the Geological Society, 163*(2006), 707-721.

Galloway, W. (1998). Siliciclastic slope and base-of-slope depositional systems: component facies, stratigraphic architecture, and classification. *AAPG Bulletin, 82*, 569-595.

García Morabito, E., & Ramos, V. A. (2012). Andean evolution of the Aluminé fold and thrust belt, Northern Patagonian Andes (38°30'–40°30'S). *Journal of South American Earth Sciences, 38*, 13-30. doi: 10.1016/j.jsames.2012.03.005

Gardner, M. H., & Borer, J. M. (2000). Submarine channel architecture along a slope to basin profile Brushy Canyon Formation, West Texas *in* A.H. Bouma and C.G. Stone, eds. Fine-grained turbidite systems. *AAPG Memoir, 68*, 195-214.

Grimaldi, G. O., & Dorobek, S. L. (2011). Fault framework and kinematic evolution of inversion structures: Natural examples from the Neuquén Basin, Argentina. *AAPG Bulletin, 95*(1), 27-60. doi: 10.1306/06301009165

Gulisano, C., & Gutierrez Pleimling, A. (1994). *Field trip guidebook, Neuquina Basin, Mendoza Province.* Paper presented at the Fourth International Congress on Jurassic Stratigraphy and Geology.

Haughton, P., Davis, C., McCaffrey, W., & Barker, S. (2009). Hybrid sediment gravity flow deposits – Classification, origin and significance. *Marine and Petroleum Geology, 26*(10), 1900-1918. doi: 10.1016/j.marpetgeo.2009.02.012

Haughton, P. D. W., Barker, S. P., & McCaffrey, W. D. (2003). 'Linked' debrites in sand-rich turbidite systems - origin and significance. *Sedimentology, 50*, 459-482.

Hesse, R. (1995). Long-distance correlation of spill-over turbidites on the western levee of the Northwest Atlantic Mid-Ocean Channel (NAMOC), Labrador Sea. *Atlas of Deep-Water Environments: Architectural Style in Turbidite Systems: London, Chapman & Hall*, 276-281.

Hodgson, D. M. (2009). Distribution and origin of hybrid beds in sand-rich submarine fans of the Tanqua depocentre, Karoo Basin, South Africa. *Marine and Petroleum Geology, 26*(10), 1940-1956. doi: 10.1016/j.marpetgeo.2009.02.011

Ito, M. (2008). Downfan Transformation from Turbidity Currents to Debris Flows at a Channel-to-Lobe Transitional Zone: The Lower Pleistocene Otadai Formation, Boso Peninsula, Japan. *Journal of Sedimentary Research, 78*(10), 668-682. doi: 10.2110/jsr.2008.076

Jackson, C. A. L., Zakaria, A. A., Johnson, H. D., Tongkul, F., & Crevello, P. D. (2009). Sedimentology, stratigraphic occurrence and origin of linked debrites in the West Crocker Formation (Oligo-Miocene), Sabah, NW Borneo. *Marine and Petroleum Geology, 26*(10), 1957-1973. doi: 10.1016/j.marpetgeo.2009.02.019

Johannessen, E. P., & Steel, R. J. (2005). Shelf-margin clinoforms and prediction of deepwater sands. *Basin Research, 17*(4), 521-550. doi: 10.1111/j.1365-2117.2005.00278.x

Johnson, S., Flint, S., Hinds, D., & De Ville Wickens, H. (2001). Anatomy, geometry and sequence stratigraphy of basin floor to slope turbidite systems, Tanqua Karoo, South Africa. *Sedimentology, 48*, 987-1023.

Kane, I. A., & Ponten, A. S. M. (2012). Submarine transitional flow deposits in the Paleogene Gulf of Mexico. *Geology, 40*(12), 1119-1122. doi: 10.1130/g33410.1

Kneller, B., & Branney, M. J. (1995). Sustained high-density turbidity currents and the deposition of thick massive sands. *Sedimentology, 42*, 607-616.

Kochhann, K. G. D., Baecker-Fauth, S., Pujana, I., Santos da Silveira, A., & Fauth, G. (2011). Toarcian–Aalenian (Early–Middle Jurassic) radiolarian fauna from the Los Molles Formation, Neuquén Basin, Argentina: Taxonomy and paleobiogeographic affinities. *Journal of South American Earth Sciences, 31*(2-3), 253-261. doi: 10.1016/j.jsames.2011.01.001

Komar, P. D. (1971). Hydraulic Jump in turbidity currents. *GSA Bulletin, 82*, 1477-1488.

Legarreta, L., & Uliana, M. A. (1996). The Jurassic succession in west-central Argentina: stratal patterns, sequences and paleogeographic evolution. *Palaeogeography, Palaeoclimatology, Palaeoecology, 120*, 303-330.

Lowe, D. R. (1982). Sediment gravity flows: II. depositional models with special reference to the deposits of high-density turbidity currents. *Journal of Sedimentary Petrology, 52*(1), 0279-0297.

Lucchi, F. R., & Valmori, E. (1980). Basin-wide turbidites in a Miocene, over-supplied deep-sea plain: a geometrical analysis. *Sedimentology, 27*, 241-270.

Martinez, M. A., Pramparo, M. B., Quattrocchio, M. E., & Zavala, C. (2008). Depositional environments and hydrocarbon potential of the Middle Jurassic Los Molles Formation, Neuquen Basin, Argentina: palynofacies and organic geochemical data. *Revista Geologica de Chile, 2*(35), 279-305.

Middleton, G. (1967). Experiments on density and turbidity currents III. Deposition of sediment. *Canadian Journal of Earth Sciences, 4*.

Middleton, G., & Hampton, M. A. (1973). Sediment gravity flows: mechanics of flow and deposition.

Mohrig, D., Elverhøi, A., & Parker, G. (1999). Experiments on the relative mobility of muddy subaqueous and subaerial debris flows, and their capacity to remobilize antecedent deposits. *Marine Geology, 154*(1), 117-129.

Morgans-Bell, H. S., & McIlroy, D. (2005). Palaeoclimatic implications of Middle Jurassic (Bajocian) coniferous wood from the Neuquen Basin, west-central Argentina. *Geological Society, London, Special Publications, 252*(1), 267-278. doi: 10.1144/gsl.sp.2005.252.01.13

Mulder, T., & Alexander, J. (2001). The physical character of subaqueous sedimentary density flows and their deposits. *Sedimentology, 48*, 269-299.

Mulder, T., & Etienne, S. (2010). Lobes in deep-sea turbidite systems: State of the art. *Sedimentary Geology, 229*(3), 75-80. doi: 10.1016/j.sedgeo.2010.06.011

Muravchik, M., D'Elia, L., Bilmes, A., & Franzese, J. R. (2011). Syn-eruptive/inter-eruptive relations in the syn-rift deposits of the Precuyano Cycle, Sierra de Chacaico, Neuquén Basin, Argentina. *Sedimentary Geology, 238*(1-2), 132-144. doi: 10.1016/j.sedgeo.2011.04.008

Mutti, E. (1977). Distinctive thin-bedded turbidite facies and related depositional environments in the Eocene Hecho Group (South-central Pyrenees, Spain). *Sedimentology, 24*, 107-131.

Mutti, E., & Normark, W. R. (1991). An integrated approach to the study of turbidite systems *Seismic facies and sedimentary processes of submarine fans and turbidite systems* (pp. 75-106): Springer.

Mutti, E., & Ricci Lucchi, F. (1972). Le torbiditi dell'Appennino settentrionale: introduzione all'analisi di facies. *Mem. Soc. Geol. Ital, 11*(2), 161-199.

Naipauer, M., García Morabito, E., Marques, J. C., Tunik, M., Rojas Vera, E. A., Vujovich, G. I., . . . Ramos, V. A. (2012). Intraplate Late Jurassic deformation and exhumation in western central Argentina: Constraints from surface data and U–Pb detrital zircon ages. *Tectonophysics, 524-525*, 59-75. doi: 10.1016/j.tecto.2011.12.017

Nittrouer, J. A., Shaw, J., Lamb, M. P., & Mohrig, D. (2012). Spatial and temporal trends for water-flow velocity and bed-material sediment transport in the lower Mississippi River. *Geological Society of America Bulletin, 124*(3-4), 400-414.

Olariu, M. I., Aiken, C. L. V., Bhattacharya, J. P., & Xu, X. (2011). Interpretation of channelized architecture using three-dimensional photo real models, Pennsylvanian deep-water deposits at Big Rock Quarry, Arkansas. *Marine and Petroleum Geology, 28*(6), 1157-1170. doi: http://dx.doi.org/10.1016/j.marpetgeo.2010.12.007

Olariu, M. I., Ferguson, J. F., & Aiken, C. L. V. (2008). Outcrop fracture characterization using terrestrial laser scanners: Deep-water Jackfork sandstone at Big Rock Quarry, Arkansas. [Article]. *Geosphere, 4*(1), 247-259. doi: 10.1130/ges00139.1

Oliveira, C. M. M., Hodgson, D. M., & Flint, S. S. (2011). Distribution of soft-sediment deformation structures in clinoform successions of the Permian Ecca Group, Karoo Basin, South Africa. *Sedimentary Geology, 235*(3-4), 314-330. doi: 10.1016/j.sedgeo.2010.09.011

Paim, P. S. G., Silveira, A., Lavina, E., Faccini, U., Leanza, H., Teixeira de Oliveira, J. M. M., & D'avila, R. (2008). High resolution stratigraphy and gravity flow deposits in the Los Molles Formation (Cuyo Group - Jurassic) at La Jardinera Region, Neuquen Basin. *Revista de la Asociacion Geologica Argentina, 63*, 728-753.

Palanques, A., Kenyon, N., Alonso, B., & Limonov, A. (1995). Erosional and depositional patterns in the Valencia Channel mouth: an example of a modern channel-lobe transition zone. *Marine Geophysical Researches, 17*(6), 503-517.

Piper, D. (1970). Transport and deposition of Holocene sediment on La Jolla deep sea fan, California. *Marine Geology, 8*(3), 211-227.

Posamentier, H. W. (2003). Depositional elements associated with a basin floor channel-levee system: case study from the Gulf of Mexico. *Marine and Petroleum Geology, 20*(6-8), 677-690. doi: 10.1016/j.marpetgeo.2003.01.002

Poulos, S. E., Collins, M.B, Pattiaratchi, C., Cramp, A., Gull, A. Tsimplis, M., Papatheodorou, G. (1996). Oceanography and sedimentation in the semi-enclosed, deep-water Gulf of Corinth (Greece). *Marine Geology, 134*, 213-235.

Prelat, A., & Hodgson, D. M. (2013). The full range of turbidite bed thickness patterns in submarine lobes: controls and implications. *Journal of the Geological Society, 170*(1), 209-214. doi: 10.1144/jgs2012-056

Prelat, A., Hodgson, D. M., & Flint, S. S. (2009). Evolution, architecture and hierarchy of distributary deep-water deposits: a high-resolution outcrop investigation from the Permian Karoo Basin, South Africa. *Sedimentology, 56*(7), 2132-2154. doi: 10.1111/j.1365-3091.2009.01073.x

Pyrcz, M. J., Catuneanu, O., & Deutsch, C. V. (2005). Stochastic surface-based modeling of turbidite lobes. *AAPG Bulletin, 89*(2), 177-191. doi: 10.1306/09220403112

Pyrcz, M. J., & Deutsch, C. V. (2014). *Geostatistical reservoir modeling*: Oxford University Press.

Ramos, V. A. (2008). Patagonia: A paleozoic continent adrift? *Journal of Sedimentary Research*(26), 235-251.

Riccardi, A. C., Leanza, H. A., Damborenea, S. E., Mancenido, M. O., Ballent, S. C., & Zeiss, A. (2000). Marine mesozoic biostratigraphy of the nenquen basio. *Zeitschrift für angewandte Geologie*, 103-108.

Shanmugan, G. (2006). Deep-water processes and facies models: implications for sandstone petroleum reservoirs.

Shaw, J. B., Mohrig, D., & Whitman, S. K. (2013). The morphology and evolution of channels on the Wax Lake Delta, Louisiana, USA. *Journal of Geophysical Research: Earth Surface, 118*(3), 1562-1584.

Sinclair, H. D., & Cowie, P. A. (2003). Basin-Floor Topography and the Scaling of Turbidites. *The Journal of Geology, 111*, 277-299.

Smith, R., & Spalletti, L. (1995). Erosional, depositional and post-depositional features of a turbidite channel-fill: Jurassic of the Neuquén basin, Argentina. ln: Atlas of Deep Water Environments: Architectural Style in Turbidity Systems (K. Pickering, R. Hiscott. N. Kenyon, F. Ricci Lucchi. y R. Smith, Eds.): Chapman and Hall, London.

Steel, R., & Olsen, T. (2002). Clinoforms, clinoform trajectories and deepwater sands. In: Sequence Stratigraphic Models for Exploration and Production: Evolving Methodology, Emerging Models and Applications Histories (Eds J.M. Armentrout and N.C. Rosen). *Gulf Coast Section SEPM Proc. 22nd Annu. Res. Conf.*, 367-380.

Stelting, C. E., Bouma, A. H., & Stone, C., G. (2000). Fine-grained turbidite systems (AAPG Memoir 72-SEPM Special Publication 68).pdf>. *AAPG Memoir 72, SEPM Special Publication 68*.

Sumner, E. J., Talling, P. J., & Amy, L. A. (2009). Deposits of flows transitional between turbidity current and debris flow. *Geology, 37*(11), 991-994. doi: 10.1130/g30059a.1

Talling, P. J., Amy, L. A., & Wynn, R. B. (2007). New insight into the evolution of large-volume turbidity currents: comparison of turbidite shape and previous modelling results. *Sedimentology, 54*(4), 737-769. doi: 10.1111/j.1365-3091.2007.00858.x

Talling, P. J., Masson, D. G., Sumner, E. J., & Malgesini, G. (2012). Subaqueous sediment density flows: Depositional processes and deposit types. *Sedimentology, 59*(7), 1937-2003. doi: 10.1111/j.1365-3091.2012.01353.x

Uroza, C. A., & Steel, R. J. (2008). A highstand shelf-margin delta system from the Eocene of West Spitsbergen, Norway. *Sedimentary Geology, 203*(3-4), 229-245. doi: 10.1016/j.sedgeo.2007.12.003

Vann, N. K. (2013). Slope to basin floor evolution of channels to lobes, Jurassic Los Molles Formation, Neuquen Basin, Argentina. *Thesis for the Masters Degree in Stratigraphy/Sedimentology, Department of Geological Science The University of Texas at Austin, USA*.

Vergani, G. D., Tankard, A. J., Belotti, H. J., & Welsink, H. J. (1995). Tectonic evolution and paleogeography of the Neuquen Basin, Argentina *AAPG Memoir, 62*, 383-402.

Walker, R. G., & James, N. P. (1992). *Facies models: response to sea level change* (Vol. 1): Geological Assn of Canada.

Wynn, R. B., Kenyon, N. H., Masson, D. G., Stow, D., A. V., & Weaver, P. P. E. (2002). *Characterization and recognition of deep-water channel-lobe transition zones*.

Zavala, C. (1996). Sequence stratigraphy in continental to marine transitions. An example from the Middle Jurassic Cuyo Group, South Neuquen Basin, Argentina. *GeoResearch Forum, 1-2*, 285-294.